AD/A-005 057

LITHIUM-INORGANIC ELECTROLYTE
BATTERIES

Gerhard L. Holleck, et al

EIC, Incorporated

Prepared for:

Army Electronics Command

January 1975

REPORT DOCUMENTATION PAGE		READ INSTRUCTIONS BEFORE COMPLETING FORM
1. REPORT NUMBER ECOM-74-0030-4	2. GOVT ACCESSION NO.	3. RECIPIENT'S CATALOG NUMBER AD/A-005057
4. TITLE (and Subtitle) LITHIUM - INORGANIC ELECTROLYTE BATTERIES		5. TYPE OF REPORT & PERIOD COVERED Annual Summary Report 17 Sep 1973 - 16 Sep 1974 6. PERFORMING ORG. REPORT NUMBER C-401
7. AUTHOR(s) Gerhard L. Holleck, Michael J. Turchan and David R. Cogley		8. CONTRACT OR GRANT NUMBER(s) DAAB07-74-C-0030
9. PERFORMING ORGANIZATION NAME AND ADDRESS EIC, Inc. 55 Chapel Street, Newton, Ma. 02158		10. PROGRAM ELEMENT, PROJECT, TASK AREA & WORK UNIT NUMBERS 1T1 61102 A34A 02435
11. CONTROLLING OFFICE NAME AND ADDRESS U.S. Army Electronics Command Attn: AMSEL-TL-P Fort Monmouth, N.J. 07703		12. REPORT DATE JANUARY 1975 13. NUMBER OF PAGES 58
14. MONITORING AGENCY NAME & ADDRESS(if different from Controlling Office)		15. SECURITY CLASS. (of this report) Unclassified 15a. DECLASSIFICATION/DOWNGRADING SCHEDULE

16. DISTRIBUTION STATEMENT (of this Report)

Approved for Public Release; distribution unlimited.

17. DISTRIBUTION STATEMENT (of the abstract entered in Block 20, if different from Report)

18. SUPPLEMENTARY NOTES

19. KEY WORDS (Continue on reverse side if necessary and identify by block number)

Carbon Black Cathodes, Cells Utilizing Solvent Reduction, Inorganic
Electrolytes, Lithium Anodes, $LiAlCl_4$, Thionyl Chloride, $SOCl_2$,
Storage Effects, Temperature Effects, Reaction Mechanism.

20. ABSTRACT (Continue on reverse side if necessary and identify by block number)

An all-inorganic electrolyte, lithium primary battery operable over
the temperature range -40° to +160°F is being evaluated. The desired
energy density is 150 watt-hours per pound of total battery weight and
the desired power density is 50 watts per pound.

PRICES SUBJECT TO CHANGE.

20. Abstract (Cont.)

The discharge voltage is greater than 3.0 V and is constant over most of the battery discharge at room temperature and at 160°F. The discharge voltage and capacity are significantly less at -40°F than at room temperature; however, the low temperature performance of this battery compares very favorably with other battery systems. At all temperatures, capacity is limited by polarization of the carbon electrode.

Extended storage at room temperature leads to transitory voltage delays upon discharge, followed by rapid recovery. Prolonged storage at 160°F results in severe voltage delays and lower steady-state discharge voltages upon discharge at room temperature. Both the voltage delays and the lower discharge voltages are attributable to polarization of the Li electrode.

Corrosion of Li in $SOCl_2$ is more severe in practical stainless steel cells than in glass containers under high purity conditions. A modest pressure rise is observed on storage at 160°F. However, pressure build-up is not expected to be a problem in practical cells.

Reduction of $SOCl_2$ on Ni, stainless steel, or C is a complex, potential dependent process. Surface layers which interfere with reduction of $SOCl_2$ are formed at potentials less than 2.0 V vs. Li. Electrode passivity (in the above sense) was observed with all electrodes. LiCl is a major constituent of electrode surface films formed upon reduction in $SOCl_2/LiAlCl_4$ solutions.

Carbon is a better catalyst than Ni or stainless steel for $SOCl_2$ reduction. Significant reduction rates are observed on C even below 1.0 V vs. Li, that is, within the passive region. Lithium is passive towards $SOCl_2$ reduction. The main constituent of the surface film on Li in $SOCl_2$ is LiCl. However, evidence is presented suggesting that protection of Li against $SOCl_2$ attack is provided by some surface film other than LiCl.

Chemical analysis showed that one equivalent of LiCl is generated for each equivalent of Li oxidized. The LiCl precipitates nearly exclusively in the carbon electrode. The weight gain of the carbon electrode was due solely to LiCl precipitation. Sulfur is also a reaction product of Li/$SOCl_2$ cells. Results indicate that as much as 38% of the total sulfur of the reacted $SOCl_2$ is found as elemental sulfur. Indirect evidence points to SO_2 as a further reaction product. Both S and SO_2 are quite soluble in the electrolyte, and this complicates their quantitative determination.

TABLE OF CONTENTS

LIST OF FIGURES

LIST OF FIGURES
(Continued)

v

LIST OF TABLES

I. INTRODUCTION

In recent years there has been considerable research and development on ambient temperature, high energy density lithium cells. A particularly promising system is based on thionyl chloride, $SOCl_2$ (1). In this case, $SOCl_2$ serves both as solvent and depolarizer for the cell. The performance of $SOCl_2$ cells is impressive. For example, even though unoptimized, $Li/LiAlCl_4-SOCl_2$/carbon black cells deliver $\sim$75 Whr/lb and 40 W/lb at the 1.8 hour rate. As usual, even higher energy densities are obtained at slower discharge rates.

The purpose of the present program is to study the feasibility of an all-inorganic electrolyte lithium primary battery operable and storable over the temperature range of $-40°F$ to $+160°F$. The desired energy density is 150 watt-hours per pound of total battery weight and the desired power density is 50 watts per pound.

The present report summarizes the work carried out from September 1973 to September 1974. It contains data on the discharge behavior and performance of fresh and aged cells at various temperature, on Li corrosion and film formation, and on the cell stoichiometry. Additional data and more detail is contained in the Quarterly Reports.

During the first quarter discharge characteristics of $Li/LiAlCl_4-SOCl_2/C$ cells were obtained at ambient temperature and pressure for a variety of carbon loadings; two different types of $LiAlCl_4$ electrolyte; a range of $SOCl_2$ to C ratios; a range of current densities; and for storage times up to 23 days. A sealed cell was tested in a discharge at 160°F with monitoring of cell internal temperature, pressure, current, cell voltage, and potentials of both electrodes. Carbon electrode performance values and $SOCl_2$ utilization were determined.

In the second quarter we investigated discharge characteristics after ambient temperature storage in purified electrolytes with and without addition of candidate reaction products and possible adventitious impurities. Cell performance was characterized at 160°F and -40°F and analytical work was begun to determine the reaction stoichiometry.

The Third Quarterly Report contains data on the effect of high temperature storage, especially with respect to discharge performance and pressure generation. The film formation on Li and also on other construction materials and some of its characteristics were investigated. Further analytical procedures for sulfur were developed and used in the continued effort to determine the reaction stoichiometry.

II.   EXPERIMENTAL

A.   Materials

Materials used in the study of the Li/SOCl$_2$-LiAlCl$_4$/C system were obtained as follows:

The first carbon black used in the manufacture of the positive electrodes was purchased from Ashland Chemical Company; XC-6310-4. This material was subsequently substituted by a 50% compressed acetylene black made by Shawinigan Products Corporation which produced finished cathodes of a higher mechanical stability. The electrode binder was TFE in dispersion form, Type 30, obtained from DuPont de Nemours & Company. The negative electrode was fabricated using 15 mil thick Li metal foil obtained from Foote Mineral Company. Both electrodes were manufactured using an expanded metal screen of pure nickel as a substrate and current collector. The screen was 5 Ni 7 - 4/0 obtained from the Exmet Corporation.

The separator material used in the vast majority of cells was a glass filter paper consisting of a mat of 1 micron borosilicate glass fibers in a nonwoven configuration. The total thickness of the glass fiber material is approximately 8 mils. This was supplied by either Whatman Filter (#GF/A) or Gelman Instrument Company (part #61701).

The solvent-electrolyte system consisted of 1.8 M LiAlCl$_4$ in SOCl$_2$. Anhydrous LiAlCl$_4$ was obtained from Foote Mineral Company. LiCl from Alfa Chemical Company and AlCl$_3$ from Fluka A.G. were used to formulate a laboratory grade of LiAlCl$_4$. The thionyl chloride was obtained from Matheson, Coleman and Bell. Initially, the solvent-electrolyte system was prepared by drying the solvent with pieces of lithium metal foil for a period of 24 hours. All operations involving the solvent-electrolyte system and/or lithium were performed under prepurified argon gas in a Vacuum-Atmosphere's glove box which has a NaOH scrubber connected ahead of the purification system. In the case of the Foote Mineral Company LiAlCl$_4$, an appropriate amount was weighed out and added directly to the previously treated SOCl$_2$ to give a 1.8 molar concentration. This was designated Type B electrolyte. Mixing was continued until the salt dissolved. A dusky rose colored solution resulted. The so-called Type A electrolyte was prepared in a similar manner except that to the purified SOCl$_2$ was added first the LiCl in 5% stoichiometric excess and this was followed by the appropriate amount of AlCl$_3$. A tan colored solution resulted. After the preliminary testing conducted during the first quarter, only Type A electrolyte was used with the further refinement that the solvent was distilled. The distillation was carried out with a Teflon spinning-band column (Perkin-Elmer #251 Auto Annular Still) at atmospheric pressure. The column has 200 theoretical plates. A 1:1

2

reflux ratio was employed. One hundred fifty (150) ml of $SOCl_2$ (MCB, TX535-2722) were placed in the still pot. The first 25-50 ml distillate cut was discarded. The next 80-100 ml cut was retained. The pot residue was discarded.

Distilled material was stored in sealed volumetric flasks in an argon filled glove box (Vacuum-Atmospheres) until use.

B.   Electrodes

The method of fabricating the carbon cathodes used in this study was as follows:

A paste containing 81% by weight of the carbon black and 19% by weight of TFE binder was prepared. The Teflon weight is based on the fact that 59.5% of the liquid dispersion is solid material. To each gram of the carbon black TFE mixture, was added approximately 5-10 cm^3 of distilled water so as to create a workable paste. Depending on the carbon loading desired for a particular electrode, a measured quantity of this paste was spread uniformly over a pre-weighed expanded metal screen. The screen was normally cut to provide a predetermined geometrical electrode area. In addition, the expanded metal substrate was cut to provide an unused area which was an integral portion of the current collector screen and could be used as an electrical lead.

Once the mixture was weighed and placed on the substrate area to be pasted, it was spread with a stainless steel spatula to a uniform thickness. The screen and paste were then covered with Whatman #1 filter paper to wick up the excess water. This paper was selected due to its non-linting, yet absorbent characteristics. The electrodes were then placed between pieces of fresh filter paper and absorbent paper towels. This "package" was pressed at between 500 and 1,000 pounds for 60 seconds in a Carver hydraulic press. The package was then removed and the filter papers peeled away from the electrode. Electrodes were dried in an air oven at 65°C overnight. Typically, the heavily loaded, i.e., 30 mg/cm^2, electrodes exhibited a "mud flat" cracking after the drying step which was not found in the lower-loading electrodes. The electrodes were then sintered in a small tube furnace to provide them with a mechanically stable structure. This operation consisted of sintering the electrodes at 300°C for 15-20 minutes at temperature under an inert atmosphere of argon. Electrodes treated thusly were then placed in the glove box for subsequent testing.

Lithium electrodes were assembled simply by mounting a strip of the 0.015" lithium foil onto a 5 Ni 7 - 4/0 Exmet substrate cut to an appropriate size and with a portion of the metal screen cut to provide an electrical lead as described for the carbon cathode. This was carried out in the dry box, by simply placing the lithium foil over the proper nickel substrate on a 304 stainless steel plate and lightly hammering the foil into the mesh of the screen.

C.   Test Cells

Ir:tial vial cell assembly was carried out by placing the prepared lithium anode and carbon cathode, isolated from each other by the glass fiber separator, into an appropriate container. In most tests the cell containe was simply a pyrex glass vial approximately 65 mm tall with a diameter of 19 mm. The electrode package consisted of the carbon cathode separared with glass filter paper from the lithium anode. The latter was situated parallel to the cathode but in most cases folded around it to provide a configuration which utilizes both sides of the carbon electrode. A Li reference electrode was also placed close to the edge of the active electrode package. Electrodes tested in the vial cells had geometrical areas typically 0.5" by 1.5" (i.e., $0.75"^2$, i.e., 4.84 cm^2). This gave an active carbon surface area of 9.68 cm^2. The complete electrode packages were usually about 60 to 90 mils thick, depending upon the loading of the cathode and the electrode configuration.

Once the electrode package was placed into the glass vial, the electrode leads were bent over opposite sides of the container. The cell was then filled with approximately 10 cm^3, in the case of flooded tests, of the $LiAlCl_4-SOCl_2$ electrolyte described previously. The cell was covered with a polyethylene "snap-cap." This arrangement impeded solvent evaporation during either storage or discharge while allowing the electrode leads to be brought out of the cell. Contact between the polyethylene cap and the electrolyte was avoided due to their apparent incompatibility, as evidenced by the darkening of the material in the presence of $SOCl_2$.

In the case of the so-called "starved" cell tests, the configuration was achieved by cutting a 5/8" diameter Teflon rod lengthwise and inserting the two halves into a glass vial. Sufficient material was removed from the cut faces of the hemicylinders to create a somewhat rectangular space between them approximately 0.100" wide. Into this space were placed the electrodes under test and electrolyte was added to cover the electrodes The amount of electrolyte used was typically 2-3.5 cc. Sealable pressure cells to be used at temperatures other than ambient were constructed of 304 or 316 stainless steel pipe fittings. A Conax sealing assembly allowed the passage of three Teflon coated 25 mil pure nickel wires, an iron-constantan thermocouple and a pressure gage, into a cell cavity of approximately 50 cc volume. The wires were attached to the three electrodes.

During initial experiments the electrodes were wrapped in a jelly roll configuration and electrolyte was merely introduced directly into the stainless steel cell. Later experiments utilized the identical electrode configuration used in the vial cells. In addition, the electrolyte was isolated from the cell case with a glass vial inserted within the cell.

Cell temperature was maintained by placing the sealed cells in a Model SST Tenney Environmental Chamber. All cells were allowed to

equilibrate prior to discharge.

In addition to the battery configurations, standard two and three compartment cells with glass frits were also used for simple electrode studies.

D.   Test Procedure

Initial cells were discharged under constant load using a variety of precision resistors ($\pm$ 1%). The majority of cells were discharged under constant current conditions at a predetermined current density in order to easily compare data from a variety of experiments. The cell voltage, carbon electrode potential vs. the lithium reference, cell pressure, cell internal temperature and oven temperature (where applicable) were monitored during the subsequent discharge.

Potentiostatic and galvanostatic studies of $SOCl_2$ reduction on Ni, SS and vitreous carbon were carried out in cells described above, utilizing similar electrode configurations. Electrolytes used were prepared in a manner identical to that of the Type A electrolytes, the constituents and amounts varying according to the particular experiments described in the following sections. Characteristics of the film formed on the Li anode were studied utilizing the current-interrupter method. Actual measurements were collected from photographs of potential drops using a Tektronix R5103N oscilloscope with a time base which provided a suitable rapid trace speed. The current pulse was broken with a mercury relay system which triggered the oscilloscope.

E.   Analytical Procedures

Chemical analysis of discharged and partially discharged cells was conducted using standard analytical techniques. Specifically, cells were first analyzed for Li^+ and Cl^- by dismantling them after the controlled discharge, separating the components and extracting the carbon cathode with fresh distilled $SOCl_2$ to remove soluble substances such as $LiAlCl_4$. Blanks were run on undischarged cathodes immersed in the electrolyte and extracted in an identical manner. After vacuum drying the carbon electrodes, they were weighed and extracted with distilled water to remove the soluble materials. Electrodes were then dried and reweighed to determine the amount of material removed and if any material remained in the electrode.

The aqueous leachates were then analyzed for Li^+ and Cl^-. The Li^+ was determined on an Instrumentation Laboratories Model 143A flame photometer. A 1.5 mM K^+ internal standard was used for each sample. Readings for unknowns were compared with standard Li^+ solutions.

The Cl^- was determined by potentiometric titration with $AgNO_3$. The Ag sensing electrode and an Ag/AgCl reference electrode were used in a stirred, jacketed beaker thermostated at 25°C. Silver nitrate solutions were standardized against primary standard NaCl solutions. Other cell components, e.g., the separator, were analyzed in a similar manner.

5

The solubility of sulfur in thionyl chloride was determined at 23°C in the following manner. Freshly distilled $SOCl_2$ was heated to just below its boiling point and to this was added powdered sulfur (Alfa Chemical) until a precipitate formed which would not dissolve. The solution was cooled and filtered. A portion was then collected volumetrically and the $SOCl_2$ evaporated by heating from a tared container. The amount of dissolved sulfur was then determined gravimetrically. Blank tests on fresh distilled $SOCl_2$ showed no residual material present.

The solubility of sulfur in $SOCl_2$ was substantial compared to the amounts expected from any proposed reaction mechanism. Therefore, methods to extract any sulfur produced by the reaction were established. After a number of preliminary procedures were tested on known amounts of sulfur in $SOCl_2$-$LiAlCl_4$ electrolyte a satisfactory method was achieved. The method consisted of extracting the entire cell contents a minimum of five times with freshly distilled $SOCl_2$. The $SOCl_2$ was then evaporated leaving the electrolyte salts and solid reaction product. To this was added small amounts of water to react with the $LiAlCl_4$ as a precaution against any interference with the final analysis. The sample was then again dried. The residue was transferred to an extraction thimble and extracted with carbon disulfide in a Soxhlet apparatus for 4-6 hours. Aliquots of the CS_2-S solution were transferred to titration flasks and the CS_2 was evaporated.

The sulfur analysis method employed was that of Skoog and Bartlett (2). It is based on the reaction of S with CN^- to form SCN^-.

$$S_8 + 8NaCN \rightarrow 8NaSCN$$

Specifically, to the sulfur-containing flask was added an aliquot of acetone and 15 to 20% H_2O. This solution is then titrated with NaCN in isopropanol. In order for the reaction to proceed at a sufficient rate, the solution was heated close to boiling. The end point is indicated by an increase in the solution pH value, due to hydrolysis of free NaCN. This was detected using 2 drops of bromocresol purple indicator. Aliquots of reagent grade CS_2 gave the same results as 20% water-80% acetone blanks. That is, they did not react with cyanide.

Sulfur dioxide has been proposed as a possible product of the electrochemical reduction of $SOCl_2$ in this system (3). Previous literature (4) has suggested that the solubility of SO_2 in $SOCl_2$ is very low; additional literature (5) has suggested solubilities on the order of twice as high. Based on suggested reaction mechanisms and this low solubility, pressures much greater than those recorded should occur. To clarify this situation an experiment to determine the actual solubility of SO_2 in $SOCl_2$ was performed as follows: To a one liter flask a mercury manometer and manifold system were attached. The dead volume of the flask system was accurately measured. The flask was evacuated and then backfilled with one atmosphere of SO_2 after allowing for temperature equilibration. Through a rubber septum fresh distilled $SOCl_2$ was injected in measured quantities. The $SOCl_2$ was stirred with a magnetic

stirrer. From the resulting pressure decrease indicated by the manometer the solubility was then calculated. The appropriate corrections for the $SOCl_2$ vapor pressure and resultant lowered pressure of the system were made.

III. RESULTS

A. Discharge Behavior of Fresh Cells

1. Discharge at Room Temperature

A typical $Li/SOCl_2$ cell discharge is shown in Fig. 1. It is char-
acterized by an extremely flat single step voltage plateau. Using Li
reference electrodes, it was established that the potential drop at the
end of discharge is caused by the carbon electrode. The capacity was
limited by either using up the $SOCl_2$ in the electrode and in most of
the separator or by filling of the pores of the carbon electrode by a
solid which, as we will see later, has been identified as LiCl.

This conclusion is supported by the following observations:

● Discharged carbon electrodes are hard and rigid while the
original Teflon bonded carbon structure is soft and flexible.

● No additional capacity was obtained from carbon electrodes
discharged in excess electrolyte after replacing the Li electrode and
the $SOCl_2/LiAlCl_4$ electrolyte.

● Carbon electrodes can be leached out with water. A comparison
of the original electrode weight and that after water washing showed that
the solid is completely soluble. Washed electrodes are again active for
discharge in a new cell. Their performance is somewhat lower, probably
due to the apparent cracking, fissuring and a decrease in pore volume.

● Additions such as pot residue from $SOCl_2$ distillation or S_2Cl_2
have no effect on carbon electrode utilization. Large fractions of
added S_2Cl_2 (25-50%) act as a diluent and reduce cell capacity by reducing
the amount of $SOCl_2$ accessible to the carbon electrode.

● A test cell with a 50% excess of $AlCl_3$ showed a 20% capacity
increase. This agreed with the utilization of the $AlCl_3$ present in
about 4 ml of electrolyte to solubilize LiCl by the formation of $LiAlCl_4$.

● The good agreement between measured and calculated electrode
capacities.

We may estimate a limiting carbon electrode performance based on
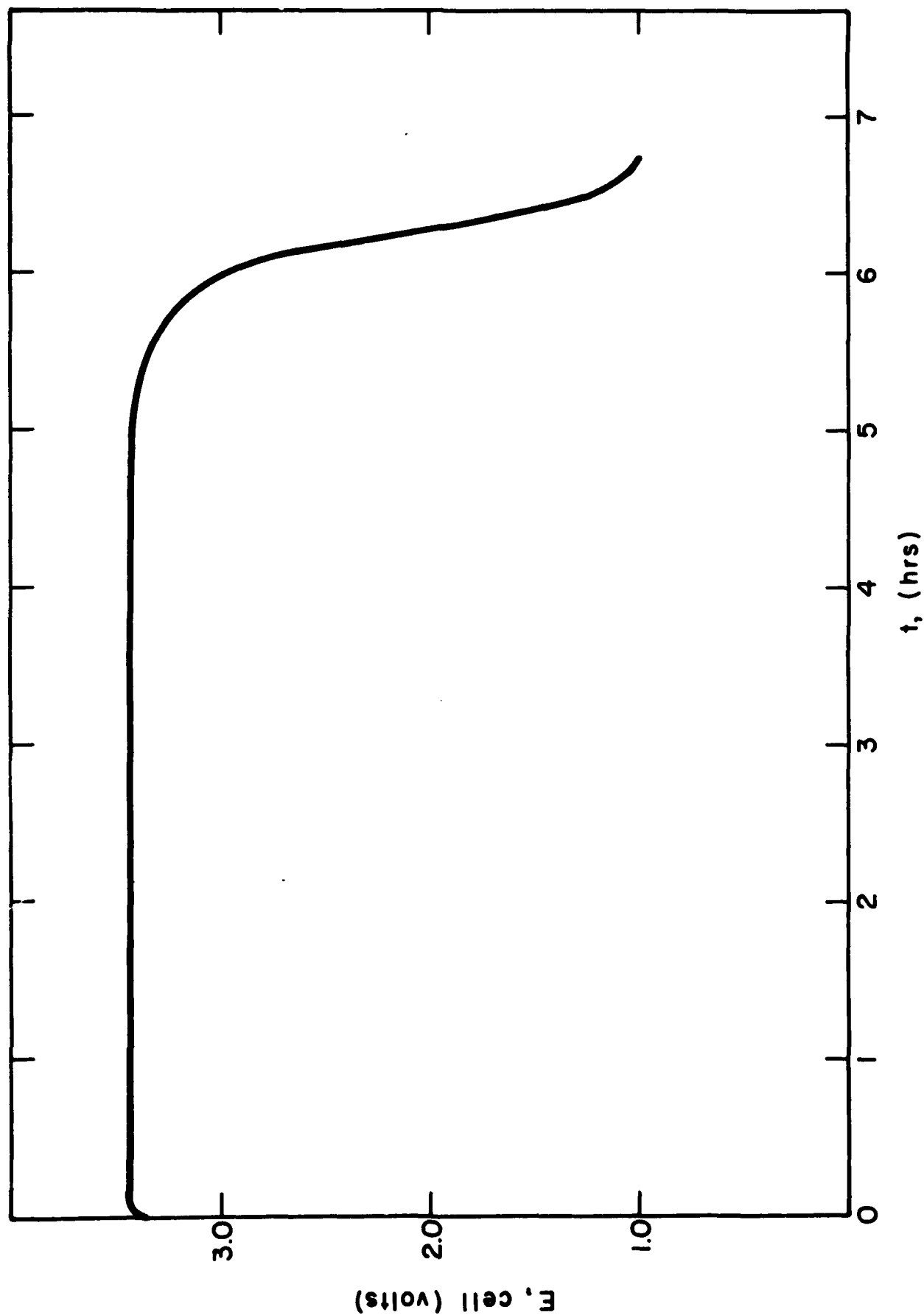the two mechanisms given above.

8

Fig. 1: Discharge Curve of Typical Fresh Cell at Room Temperature: Distilled $SOCl_2$ 1.8M $LiAlCl_4$

6

For a hypothetical infinitely thick electrode, carbon electrode performance is limited to 100% utilization of the $SOCl_2$ in the pores. For a thinner electrode, additional utilization of the $SOCl_2$ stored in the separator might be expected. Table I shows that the carbon electrodes used in our experiments had porosities of 89% independent of electrode thickness.

We may calculate the amounts of carbon and thionyl chloride corresponding to 1 cm^3 pore volume. One cm^3 pore volume corresponds to 1.124 cm^3 total volume at 89% porosity. The extra 0.124 cm^3 is carbon and Teflon, of which 81% is carbon. Using a specific gravity of 2.2 g/cm^2 for both, we calculate that there is 221 mg of carbon. Assuming a specific gravity of 1.69 grams/cm^3 for 1.8 molar $LiAlCl_4$ solution (1), one finds that the solution is 81.3% $SOCl_2$ or 1.374 g $SOCl_2/cm^3$. At 59.48 grams of $SOCl_2$ per equivalent, this leads to 0.0231 equivalent or 2229 coul. Dividing 2229 coul by the 221 mg of carbon available we obtain a theoretical carbon performance of 10.1 coul/mg carbon in a 1.8 molar $LiAlCl_4$ electrolyte with a carbon electrode which is 89% porous.

The other limiting case would consist of a free carbon electrode in excess electrolyte. Here we can calculate the maximum capacity assuming complete filling of the available pore volume with LiCl. Using the density of crystalline LiCl (2.07 g/cm^2) we find that 8.5 mg LiCl per mg C can be accommodated in our electrodes. This is equivalent to 20 coul/mg C.

Our experiments are in excellent agreement with these calculated values. For example, a 45 mil thick carbon electrode discharged at 5.7 mA/cm^2 between two Li electrodes and 8 mil separator showed a capacity of 12 coul/mg C approaching the expected limiting value of 10 coul/mg C for an infinitely thick electrode. On the contrary, 15 mil thick carbon electrodes faced by two 8 mil separators and free carbon electrodes in excess electrolyte yield capacities around 20 coul/mg C. Other electrodes showed capacities between these limiting values.

At higher current densities (>10 mA/cm^2), observed capacities are lower than the above limiting values and reflect probably a blocking of the pores at the carbon electrode surface and increased contributions of ohmic polarization in the electrolyte within the porous electrode structure. In cases where the consumption of the available $SOCl_2$ and the filling of the pore structure with LiCl are comparable in determining the cell capacity, we have also to consider the precipitation of the electrolyte salt ($LiAlCl_4$). In the limiting case where all $SOCl_2$ would react, the remaining $LiAlCl_4$ from a 1.8M solution would occupy approximately 30% of the equivalent LiCl volume. This consideration is reinforced by the recent finding that experimental cells containing 1M $LiAlCl_4$ show a larger capacity than cells containing higher electrolyte concentration (6). At lower electrolyte concentrations, the reduced

10

Table I: Carbon Electrode Porosity

Series	Total Geometric Thickness (mils)	Thickness Per Side (cm)	Volume (cm^3)	Mass (mg)	Bulk Density (mg/cm^3)	Porosity (%)
p.27	30	0.0362	.351	84	239	89
p.28	15	0.0171	.166	42	253	89
p.42 (1-6)	20	0.0235	.228	54	236	89
p.42 (7,8)	45	0.0552	.668	185	277	87

"Total geometric thickness" is the value measured from face to face with calipers. "Thickness per side" is the thickness from the electrode center to one face after correction for the equivalent screen thickness. "Volume" is the volume of the electrode not including the volume of the nickel support screen. "Mass" is the mass of the carbon and teflon. The specific gravities of carbon and teflon were taken as 2.2 g/cm^3. Nickel support screen weight was 0.294 g/geometric cm^2 which was equivalent to 1.57 mils measured face to face.

electrolyte conductivity becomes a contributing factor at practical discharge rates and, therefore, the cell capacity declines again.

2. Discharge at High Temperature

The general military high temperature specification for storage and use of batteries is 160°F (71°C) and was, therefore, also used in our experiments. A typical discharge of a fresh cell at 71°C is shown in Fig. 2. It is practically identical to that obtained at room temperature. The voltage is 3.5 V compared to 3.4 V at 25°C. Here, too, the carbon ele trode is limiting. The slight trailing of the potential towards the end of discharge is not of significance. It appears to be related to the specific cell configuration which would normally be limiting by $SOCl_2$ depletion; however, at the higher temperature excess electrolyte which was present in the cell could diffuse laterally into the cell package until voltage decay resulted from pore blocking. The pressure data during cell heat-up and discharge will be discussed later.

3. Discharge at Low Temperature

Typical discharge curves of the $Li/SOCl_2$ couple at -40°F are shown in Figs. 3 and 4.

The discharge voltage on constant load of 50Ω shows initial Li electrode polarization followed by quick (10 min) recovery to approximately 2.7 V for the first two hours, followed by a gradual voltage decrease. The carbon vs. Li reference potential parallels the cell voltage, indicating low Li anode polarization after the initial 10 minutes. Cell failure is caused by the polarization of the carbon electrode. The capacity (Fig. 3) to 1.0 V was 0.208 Ahr, equivalent to ∿40% of the value expected from similar cells at room temperature.

Another cell discharge is shown in Fig. 4. To 1.0 V, 0.187 Ahr were obtained. Then, this cell was put on open circuit and after warming to room temperature discharged further for an additional two hours at ∿2.9 V, delivering 0.149 Ahr until again the carbon electrode failed. While the cell was on open circuit, the carbon electrode potential recovers slowly, showing clearly two inflection points at approximately 2.0 and 2.9 V. The same behavior is observed if the cell is kept at -40°C, except that recovery to the original open circuit potential occurs in about six hours. This behavior, and the gradual voltage decay on discharge, suggest that reduction of $SOCl_2$ occurs in several potential-dependent steps.

In summary, approximately 40% of the room temperature capacity can be obtained at -40°F to a 1.0 V cutoff. Cell failure is caused by polarization of the carbon electrode. The carbon electrode can be discharged further if the cell is warmed to room temperature.

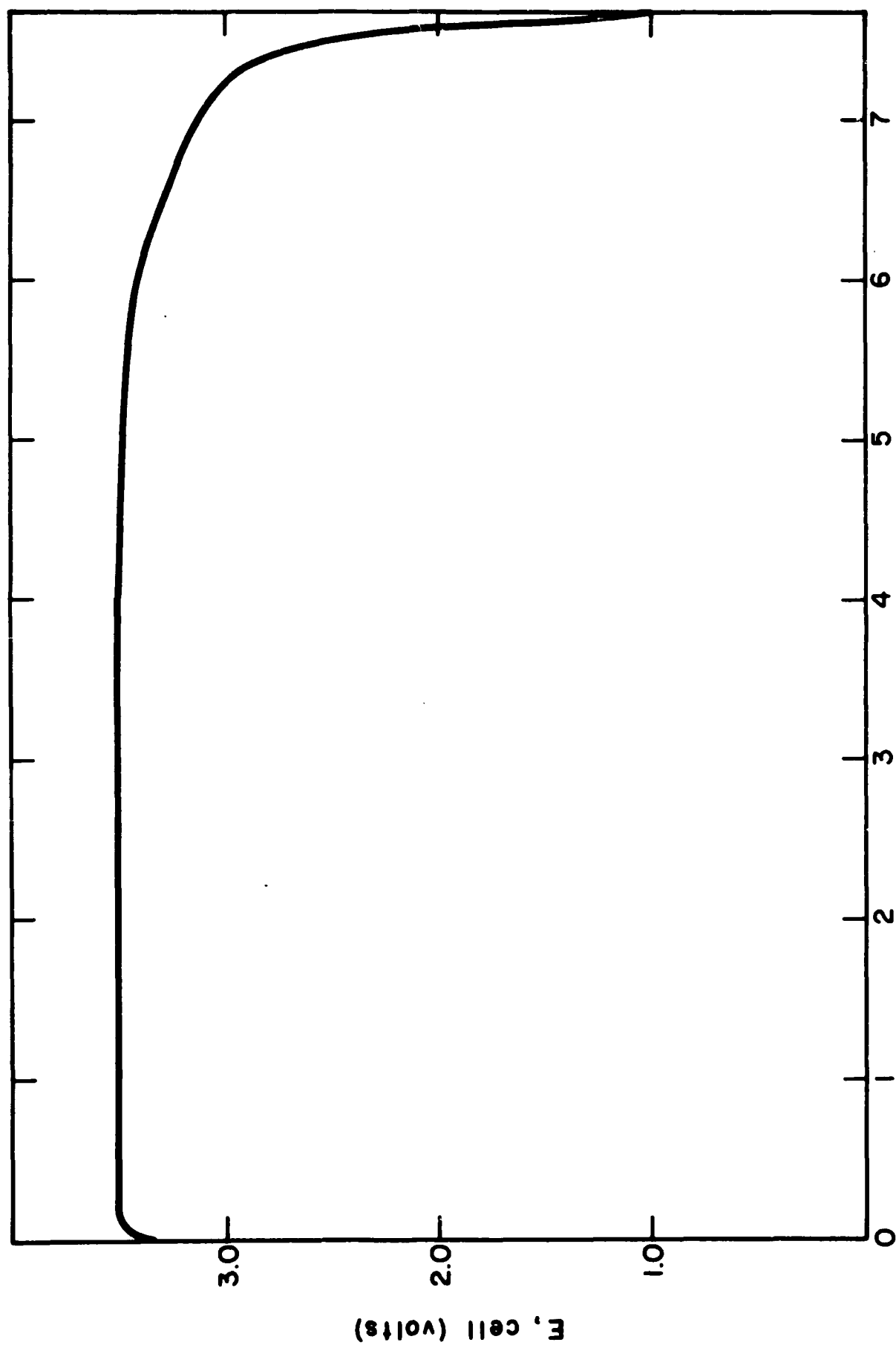Fig. 2: Discharge Curve of Typical Cell @ 160°F
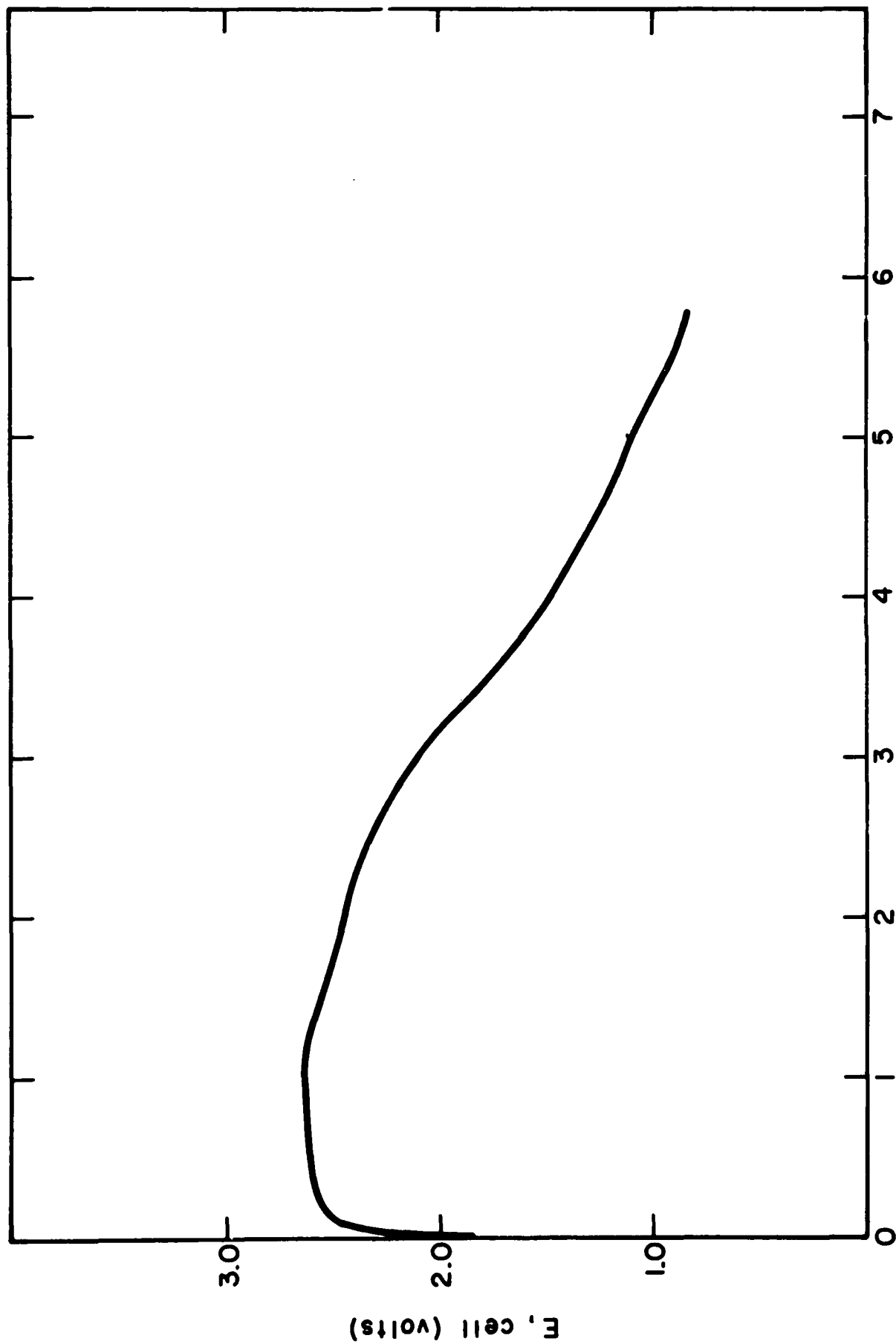
E, cell (volts)

t, (hrs)

13
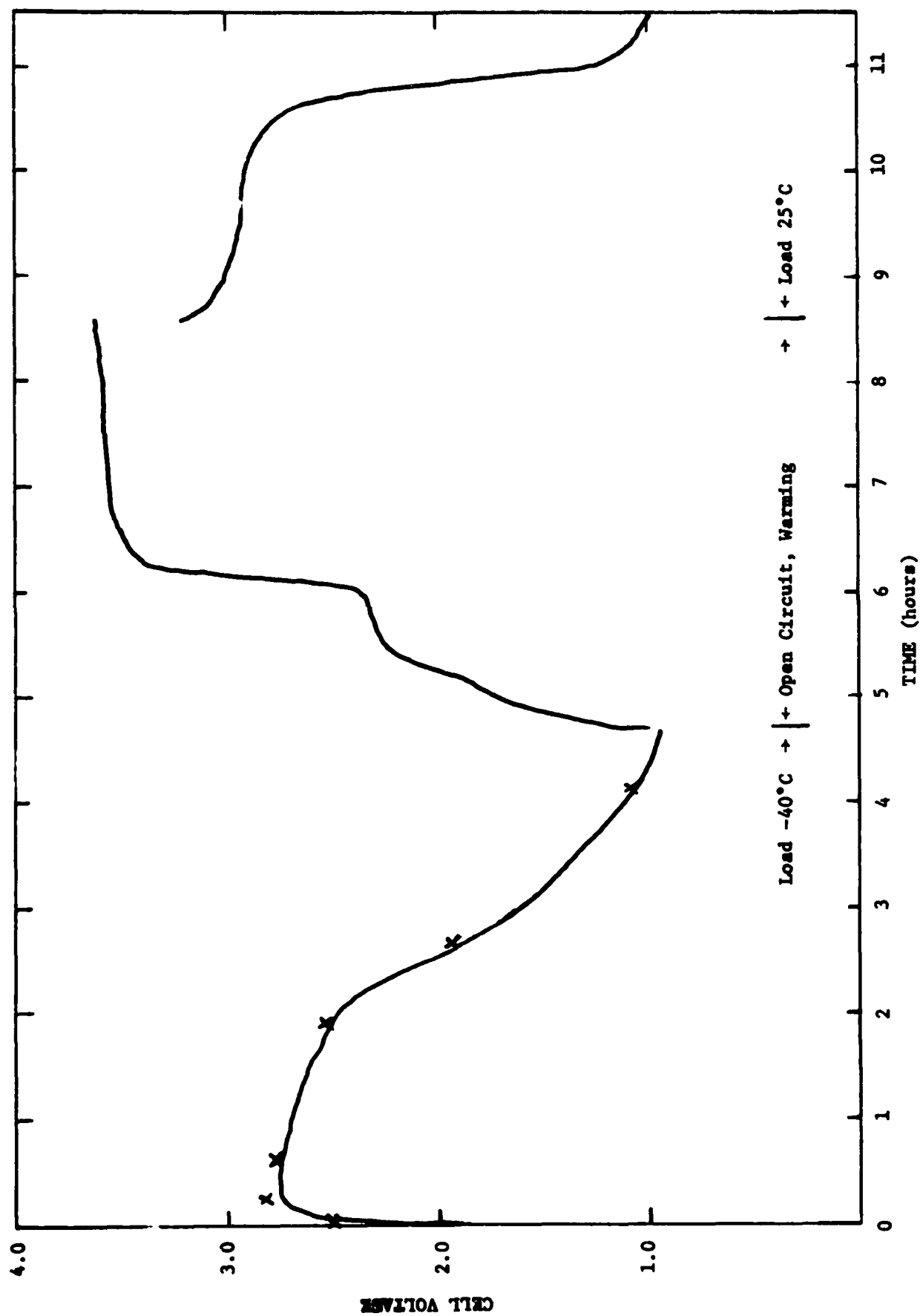
Fig. 3: Discharge Curve of Cell P-9 at -40°F

Fig. 4: Constant 50Ω Load Discharge of Cell at -40°F Followed by Further Discharge at Room Temperature. (X denotes C vs. Li reference).

15

B.   Pressure Generation in Li/SOCl$_2$ Cells

In order to determine pressure changes, many of our sealed cells were equipped with pressure gauges. Significant pressure increases on the order of 30 to 40 psi were observed only at elevated temperature (160°F). Fig. 5 shows the pressure changes during heat-up and subsequent discharge at 7-8 mA/cm^2. The observed pressures at 71°C are due in approximately equal increments to the expansion of the inert gas contained in the cell at the time of assembly, the increase in SOCl$_2$ vapor pressure (7) and a new gaseous compound. The latter must have an appreciable temperature dependent solubility since the pressure at 71°C is larger than would be expected from the final room temperature value (13 psi for the cell in Fig. 5) by consideration of vapor pressure and thermal expansion of the gas. Also, there is no direct correlation between the measured pressure and the gas space volume in the cell.

Comparable increases in cell pressure were also observed upon mere storage of cells at 71°C for extended times (see Fig. 6). Subsequent discharge of such cells at room temperature resulted in small further pressure increases. Such data are summarized in Table II. Small pressure increases (< 3 psig) were also observed upon cell discharge at -40°C.

Conclusion. The data suggest that no major product builds up in the gas phase. The data indicates further that the use of this battery will not be restricted by pressure generation, either on storage or on discharge.

C.   Reaction Stoichiometry

1.   General Consideration

Knowledge of the reaction stoichiometry is essential for the understanding of the Li/SOCl$_2$ battery system, particularly for optimization of the system with respect to energy and power density.

Several overall reactions have been proposed (3,8,9):

$$8Li + 4SOCl_2 = Li_2S_2O_4 + 6LiCl + S_2Cl_2 \tag{1}$$

$$8Li + 3SOCl_2 = Li_2SO_3 + 6LiCl + 2S \tag{2}$$

$$4Li + 2SOCl_2 = S + 4LiCl + SO_2 \tag{3}$$
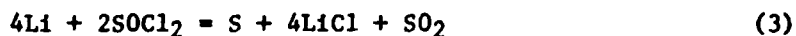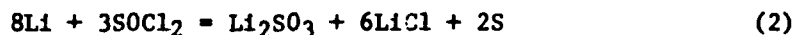
To date, it has not been established whether any of them describes fully the main reaction occurring during cell discharge.

16
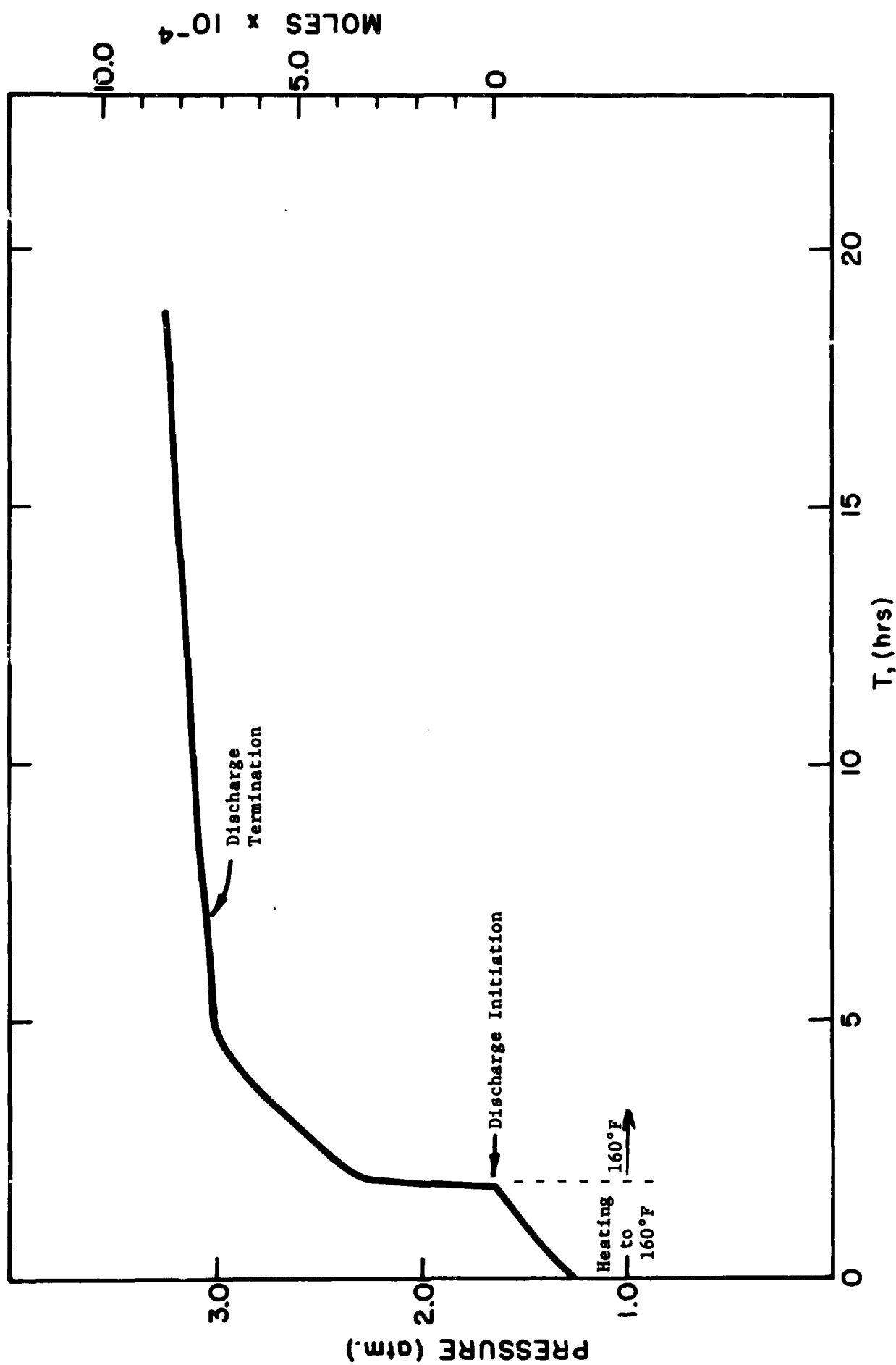
Fig. 5: Pressure Excursions of Cell P-4 While Heating to and Discharging at 160°F
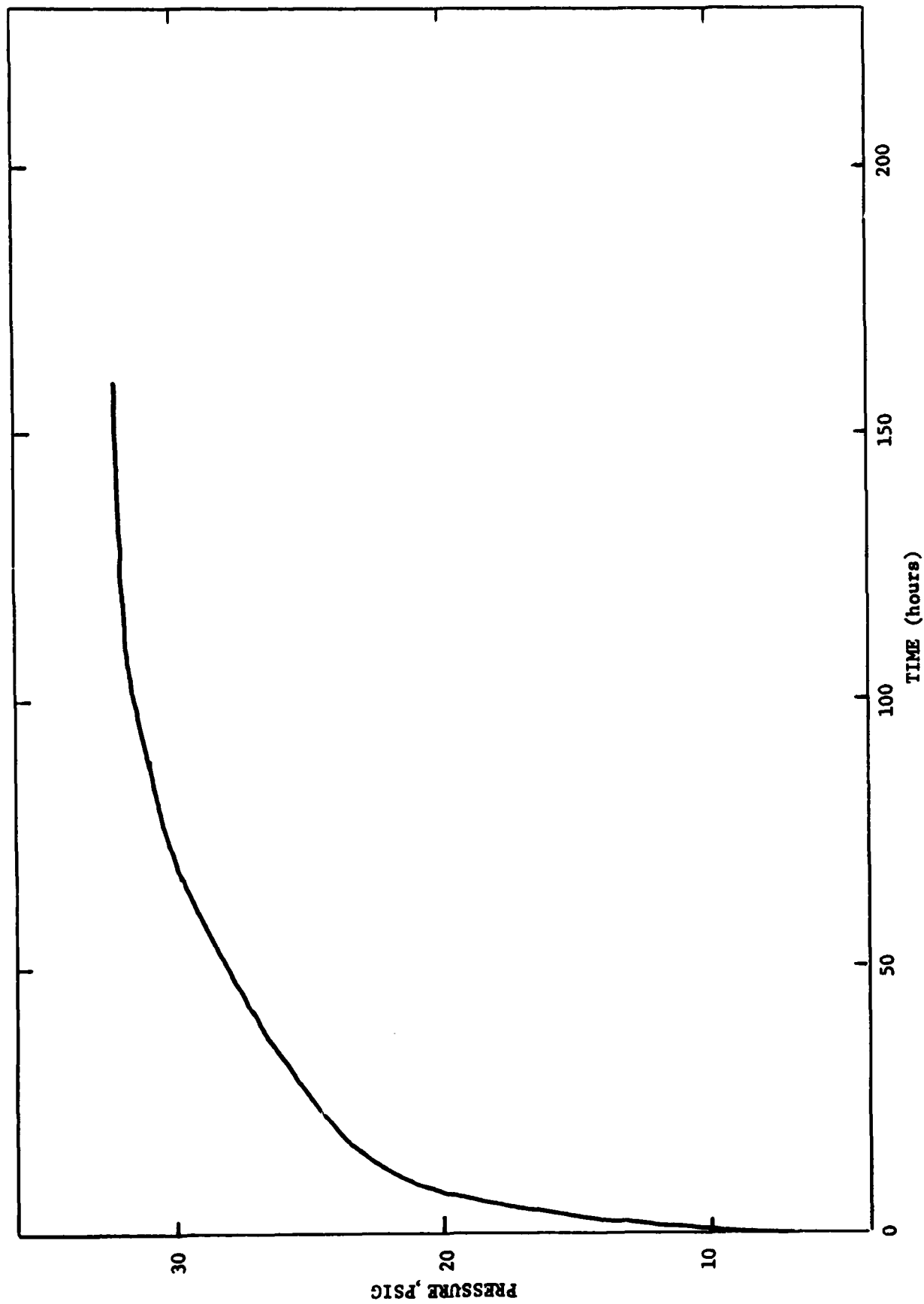
Fig. 6: Cell Pressure During Storage at 160°F

PRESSURE, PSIG

TIME (hours)

18

Table II: Pressure Data of Stores Cells, (PSIG)

Cell	Initial (R.T.)	Final P at 160°F	P, at R.T. (prior to discharge)	P, at R.T. (after discharge)
P-10 (B)	2.0	22.0	8.0*	-
P-11 (C)	5.0	32.0	9.5	11.0+
P-12 (D)	4.0	37.5	11.0	12.0
P-13A(A)	2.5	34.0	16.0	16.5

*Bad gauge

2. Analysis for Li^+ and Cl^-

Lithium chloride has been identified as a reaction product. It precipitates almost exclusively in the carbon electrode. Table III summarizes the results of the quantitative analysis for Li^+ and Cl^- in room temperature discharged cells. Li^+ and Cl^- were found in equivalent amounts. Only the first sample shows a Li^+ excess over Cl^- of 7%, exceeding the accuracy of the analysis of between 1 and 2%. The amount of LiCl is equivalent to the charge passed. In all cases, the ratio of LiCl/charge equivalent is equal or greater than one. The state of discharge has no effect on this result. As apparent from Table III, cells were discharged from 25 to 100% depth. The carbon electrode loading too had no influence on the results. A comparison of the weight gain of the carbon electrode with the LiCl found shows further that LiCl is the only solid product in the carbon electrode.

Analogous analyses were also carried out at cells operated at -40 and +71°C. This data is shown in Table IV. The results are identical to those found at room temperature, except for the amount of LiCl found in the carbon electrode per equivalent of passed charge at 71°C. The LiCl/charge ratio at 71°C was only about 0.9. The Li^+/Cl^- ratio is just at the upper limit of the experimental accuracy. At -40°C, the LiCl/charge and Li^+/Cl^- ratio are essentially one with the latter being at the low limit of the experimental accuracy.

3. Analyses for Sulfur

Various qualitative observations, especially the formation of yellow crystals after low temperature discharge suggest the formation of elemental sulfur as a reaction product. Since it was not found as a solid in the carbon electrode, it has to be appreciably soluble in the electrolyte. Our experiments showed that at room temperature the S solubility in $SOCl_2$ was 1.07M. The kinetics of elemental S dissolution at room temperature is relatively slow. At elevated temperature, S dissolves very readily at 70°C in excess of 7 mole/l.

Quantitative analysis for S in the electrolyte and in the $SOCl_2$ wash of the carbon electrode resulted in a relatively wide spread of values. The results are summarized in Table V. Up to 38% of the sulfur in $SOCl_2$ (based on a 2 electron reduction) was found as elemental sulfur. For comparison, equation (3) would suggest 50% elemental S. In order to explore the possibility of a secondary reaction of the dissolved S with the Li electrode and to possibly account for the variations in the S found, we analyzed also for sulfide ions. During these experiments it was also found that anhydrous Li_2S reacts violently with $SOCl_2$ with considerable generation of heat and evolution of gas. Elemental S is also generated during this reaction. The violence of this reaction makes it appear unlikely that Li_2S could be a stable reaction product in the

Table III: Chemical Analysis Discharged Carbon Electrodes at Room Temperature

Test	Sample	Carbon (mg)	Charge Recorded* (coul)	Charge Density (coul/mg)	Approximate % Capacity	Weight Gain** (mg)	LiCl Analysis (mg)	Li$^+$ (m moles)	Cl$^-$ (m moles)	Charge Recorded (m equiv)	Moles LiCl per Equivalent of Recorded Charge
A1	electrode	123	1670 (approx)	12.2	100	844	819	20.4	19.1	17.3 (approx)	1.14 (approx)
A2	control electrode	147	-	-	-	-	-	-	0.032	-	-
A3	separator	-	-	-	-	-	-	-	0.07	-	-
A3	electrode	117	562	4.8	40	249	242	5.75	5.66	5.82	0.98
A4	electrode	115	562	4.9	40	280	276	6.60	6.43	5.82	1.12
A5	control electrode	60	-	-	-	-	-	-	0.005	-	-
A6	electrode	60	367	6.1	(?)	171	163	3.90	3.81	3.81	1.01
A7	electrode	116	367	3.2	25	198	201	4.73	4.76	3.81	1.25
A8	electrode	60	887	14.8	(?)	399	400	9.50	9.39	9.20	1.03
A9	electrode	116	887	7.6	60	397	406	9.56	9.58	9.20	1.04

*Tests A4 and A7 may have been temporarily shorted during testing or disassembly

**Weight gain for the carbon electrodes is the weight after SOCl$_2$ washing and evacuation minus the weight of the electrode before assembly into a cell.

21

Table IV: Chemical Analysis Discharged Carbon Electrodes at -40 and +71°C

Temp.	Cell	Carbon (mg)	Charge Recorded (coul)	Charge Density (coul/mg)	Approximate % Capacity	Weight Gain * (mg)	LiCl Analysis (mg)	Li+ (m moles)	Cl- (m moles)	Charge Recorded (m equiv)	Moles LiCl per Equivalent of Recorded Charge
71°C	33	335.3	2908	8.67	100	1495.2	1147.8	26.8	27.4	30.1	0.91
71°C	58	126.7	1696	13.38	100	707.9	695.2	16.2	16.6	17.6	0.93
71°C	59	121.6	1260	10.36	100	523.1	519.3	11.9	12.6	13.06	0.94
-40°C	90	122.1	567	4.64	100	242.1	243.7	5.8	5.7	5.9	0.97
-40°C	91	123.5	315	2.55	100	143.2	137.8	3.3	3.2	3.3	0.98

*Weight gain for the carbon electrodes is the weight after $SOCl_2$ washing and evacuation minus the weight of the electrode before assembly into a cell.

22

Table V: Sulfur Analyses

Extract	Sample Cyanide Requirement (micromoles)	Sample Sulfur Content (mg)	Thionyl Chloride Reduced* (micromoles)	Fraction of Reduced Thionyl Chloride Found as Sulfur (%)
Cell 5 Lithium Electrode	50.0	1.6	-	-
Cell 5 Carbon Electrode	1,030.0	33.0	-	-
Cell 5 Total	1,080.0	34.6	4,600	23.0
Cell 6 Lithium Electrode	20.0	0.6	-	-
Cell 6 Carbon Electrode	760.0	24.4	-	-
Cell 6 Total	780.0	25.0	4,600	17.0
56.9 mg S Standard	1,775.0	56.9	-	-
Cell 58 (complete extraction)	664.6	21.3	8,787	7.5
Cell 59 (complete extraction)	2,539.7	81.4	6,528	39.0
Cell 60 (complete extraction)	2,109.1	67.6	6,202	34.5
Cell 33 (complete extraction)	2,801.8	89.8	15,067	18.5

*It is assumed that $SOCl_2$ reduction involves 2 electrons per mole.

cell environment. Further tests for other sulfur containing products and the possibility of incomplete extraction which could account for the lower S values are presently underway.

4. Properties of the Generated Gas

We have, as discussed above, observed pressure build-up in cells, especially when they are stored at elevated temperature (160°F). Pressure is generated by expansion of the residual inert gas, by $SOCl_2$ vapor, and by an as-yet unknown component. Upon cooling the gas mixture (see Fig. 7 which shows Cell I-27 A5 stored for 16 hours at 160°F and discharged 25%), a discontinuous pressure change below 0°C is observed. This suggests a condensable substance and indirect evidence points to SO_2 as a possible candidate. SO_2 has a boiling point of -10°C. The onset of gas condensation prior to this value could reflect adsorption of SO_2 onto the carbon electrode. Similar behavior was also observed with a $Li/SOCl_2-LiAlCl_4/Ni$ cell.

The measured pressure values and a reported negligible solubility in $SOCl_2$ appeared to exclude SO_2 as a major reaction product. We therefore measured the solubility of SO_2 in $SOCl_2$ and found that at room temperature a partial pressure of 0.544 atm SO_2 is in equilibrium with a 0.76M solution. At 46°C, a 0.513M solution of SO_2 in $SOCl_2$ has a SO_2 partial pressure of 0.720 atm. Thus, SO_2 was found to be quite soluble and therefore would not cause large pressure increases. Analysis by gas chromatography and cyclic voltammetry is in progress. The fact that no second step due to SO_2 reduction is observed in the discharge of $Li/SOCl_2$ cells does not exclude its presence, since at that stage the carbon electrode fails due to choking by LiCl and thus is no longer active.

5. Conclusion

We have identified LiCl, S and a gaseous component (strong evidence points to SO_2) as major reaction products during electrochemical $SOCl_2$ reduction. One equivalent of LiCl is produced for each equivalent of charge passed. The precipitation of LiCl occurs practically exclusively in the carbon electrode structure. Sulfur is soluble in the electrolyte. Quantitatively, various amounts up to 38% of the sulfur present in $SOCl_2$ were found as elemental S. Despite the relatively high solubility of SO_2 in $SOCl_2$, the observed pressure changes appear too small to accommodate all oxygen of the reduced $SOCl_2$ in the form of SO_2. Thus, in qualitative terms, equation (3) appears to be closest to the actual reaction path. In quantitative terms, we can account only for the LiCl. From the presently available data, it appears that an additional sulfur and oxygen containing species may be formed.
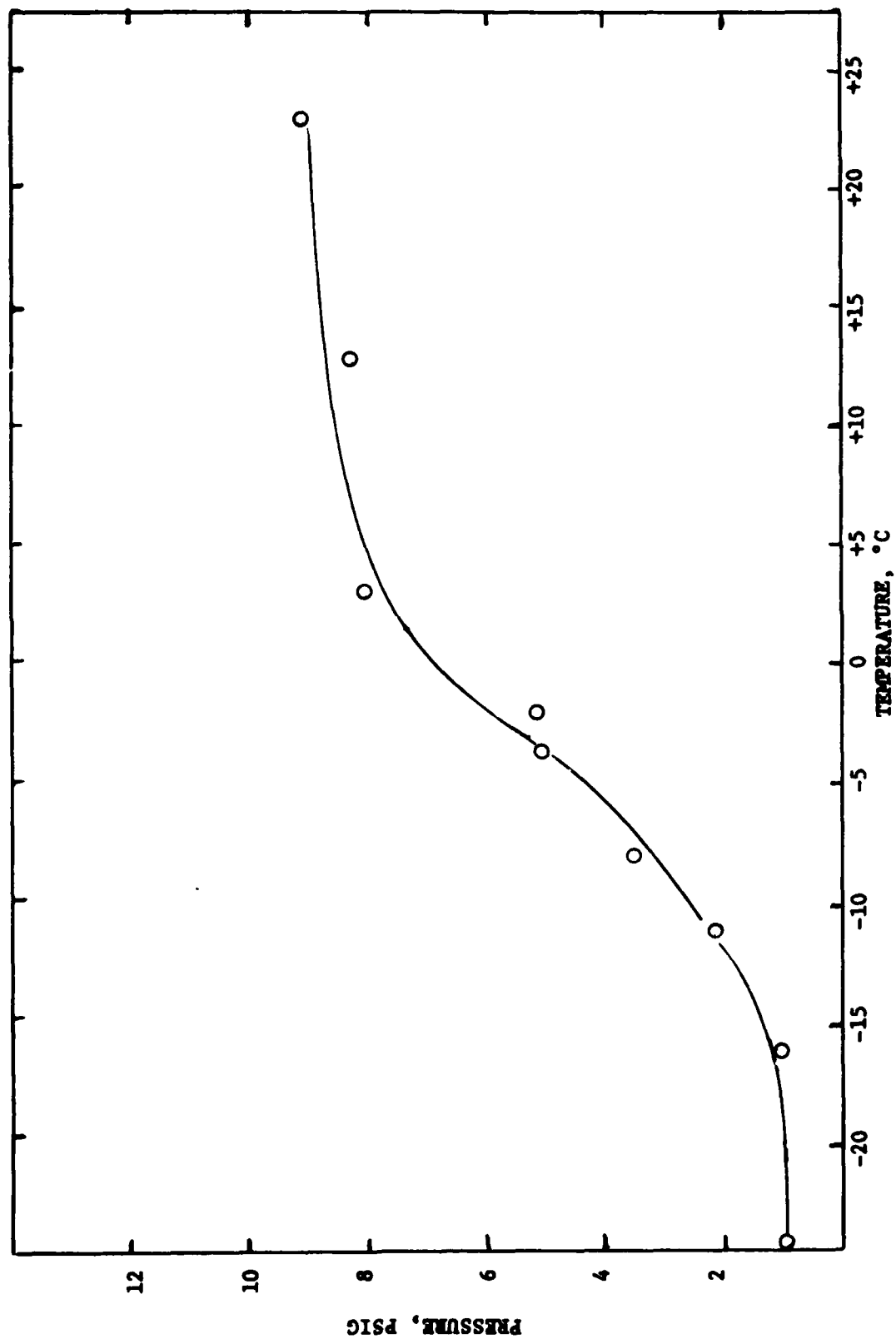
Fig. 7: Pressure of a Li/SOCl2, 1.8M LiAlCl4/C Cell as a Function of
Temperature After Storage and Partial Discharge at 160°F.

D.   Discharge Behavior of Aged Cells

1.   Room Temperature Storage

Li/SOCl$_2$ cells were stored at ambient temperature for up to 40 days.
As can be seen from the data in Table VI, there is no significant trend
of cell capacity or discharge plateau with storage time of the cells.
There was evidence for a voltage delay, however, and this polarization
increased sharply with storage time (Table VII). This delay was due
primarily to polarization of the lithium electrode, although the carbon
electrode also contributed. In all cases, the cells recovered to 95% of
their maximum voltage within a period of less than one minute. An
oscillographic trace of the voltage delay for a cell after 16 days of
storage is shown in Fig. 8.

2.   Storage at 160°F

Contrary to storage at room temperature, storage at 71°C (160°F)
followed by discharge at room temperature led to dramatic voltage delays
and reduced voltage throughout the discharge. Fig. 9 shows the discharge
of four cells after one week storage at 71°C.

All cells showed severe polarization. The cell voltage fell
extremely rapidly to very low values and then recovered somewhat, to
between 1.0 and 2.0 V. One cell did not recover at all. Measurements
against the reference electrode clearly established that in all cases the
polarization occurs at the Li electrode. Fig. 9 suggests that Type A
salts may be preferable to Type B (Foote) salts; however, we have only
one exactly comparable measurement to support such a conclusion.

Upon examination of the cells, we found that Li was very heavily
filmed during storage at elevated temperature. This resulted in heavy
salt build-up on the Li and to severe polarization during discharge.
The extent of film formation at 160°F was much greater than expected
from the experiments reported by Dey (3). We suspect that impurities,
for example, Fe originating from corrosion of the stainless steel
container, may be responsible. This implies that the stability of SOCl$_2$
batteries at 160°F may be strongly dependent on the nature and extent of
impurities introduced by materials of construction (case, screens, seals,
etc.) or even by the electrode materials themselves, particularly the
carbon paste.

Results of additional experiments carried out in glass lined
pressure vessels are shown in Figs. 10-13. Discharge of a Li/SOCl$_2$ cell
stored at 160°F for 8 days and discharged at 160°F shows a normal behavior
(Fig. 10), while galvanostatic discharge at room temperature (Fig. 12)
results in a significant polarization. The large initial polarization
(to -5.0 V) is nearly completely due to the Li electrode. However, both

Table VI: Stored Cells Using Distilled SOCl$_2$ – No Additives

Cell	Carbon Loading (mg)	Age (days)	Charge (coul)	Carbon Electrode Performance (coul/mg C)	Cell Voltage* (V)	Carbon Electrode Potential* (V)
V-20	123	0	1,494	12.2	3.40	3.37
V-22	119	8	1,500	12.6	3.32	3.35
V-24	122	14	1,735	14.2	3.30	3.30
V-26	122	22	1,609	13.2	3.25	3.32
V-31	120	30	1,505	12.5	3.32	3.30
V-35	121	40	1,433	11.8	3.25	3.25

*Cell voltage and carbon vs. Li reference potential taken at 50% of cell capacity.

Table VII: Voltage Delay with Distilled SOCl$_2$

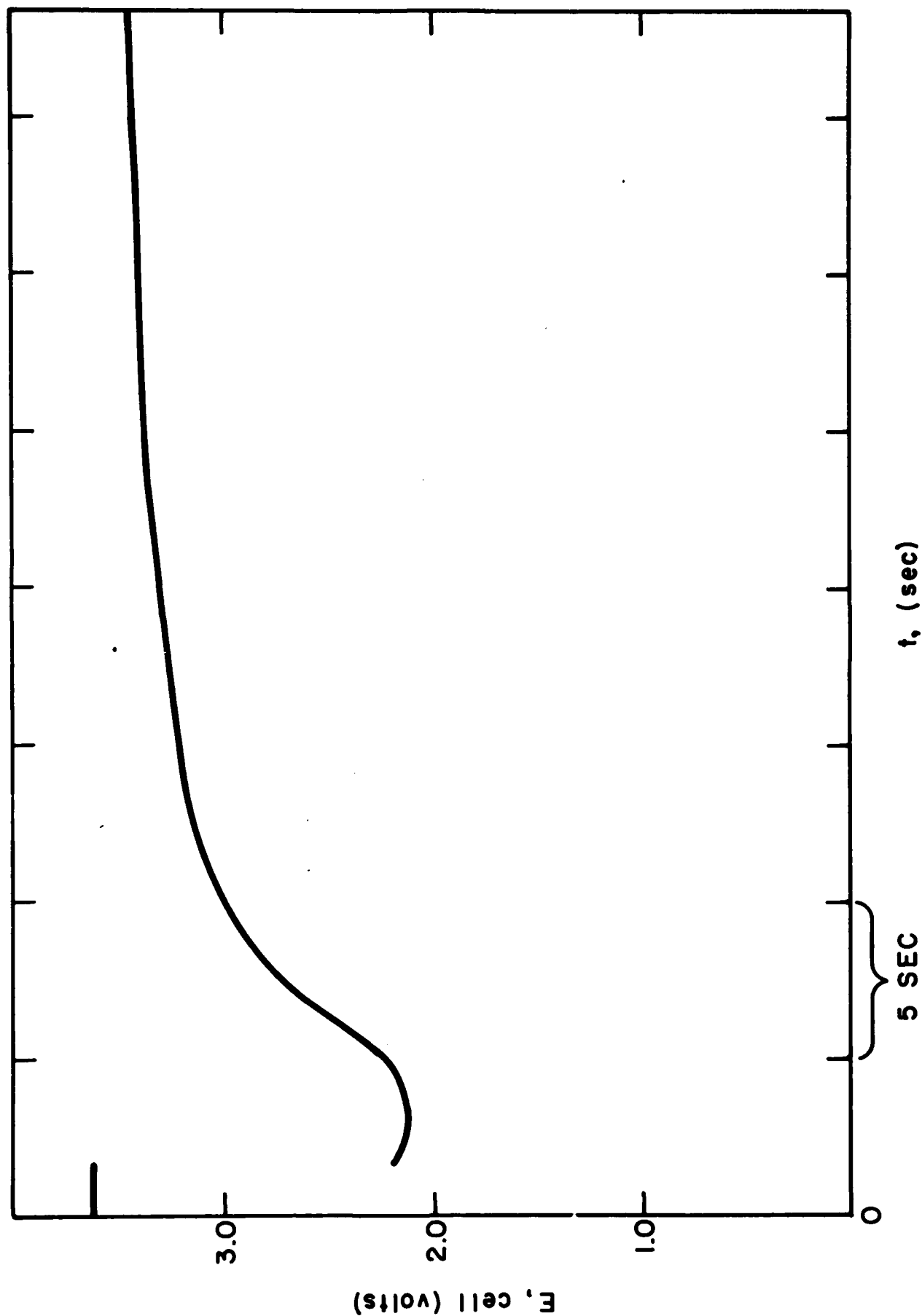| Cell	Age (days)	Cell Voltage (volts)	Carbon Electrode Potential (volts)
V-20	0	3.35	3.39
V-22	8	2.25	2.81
V-24	14	2.0	3.28
V-26	22	1.95	2.8
V-31	30	1.50	3.2
V-35	40	1.22	2.25

E, cell (volts)

t, (sec)

3.0

2.0

1.0

O

5 SEC

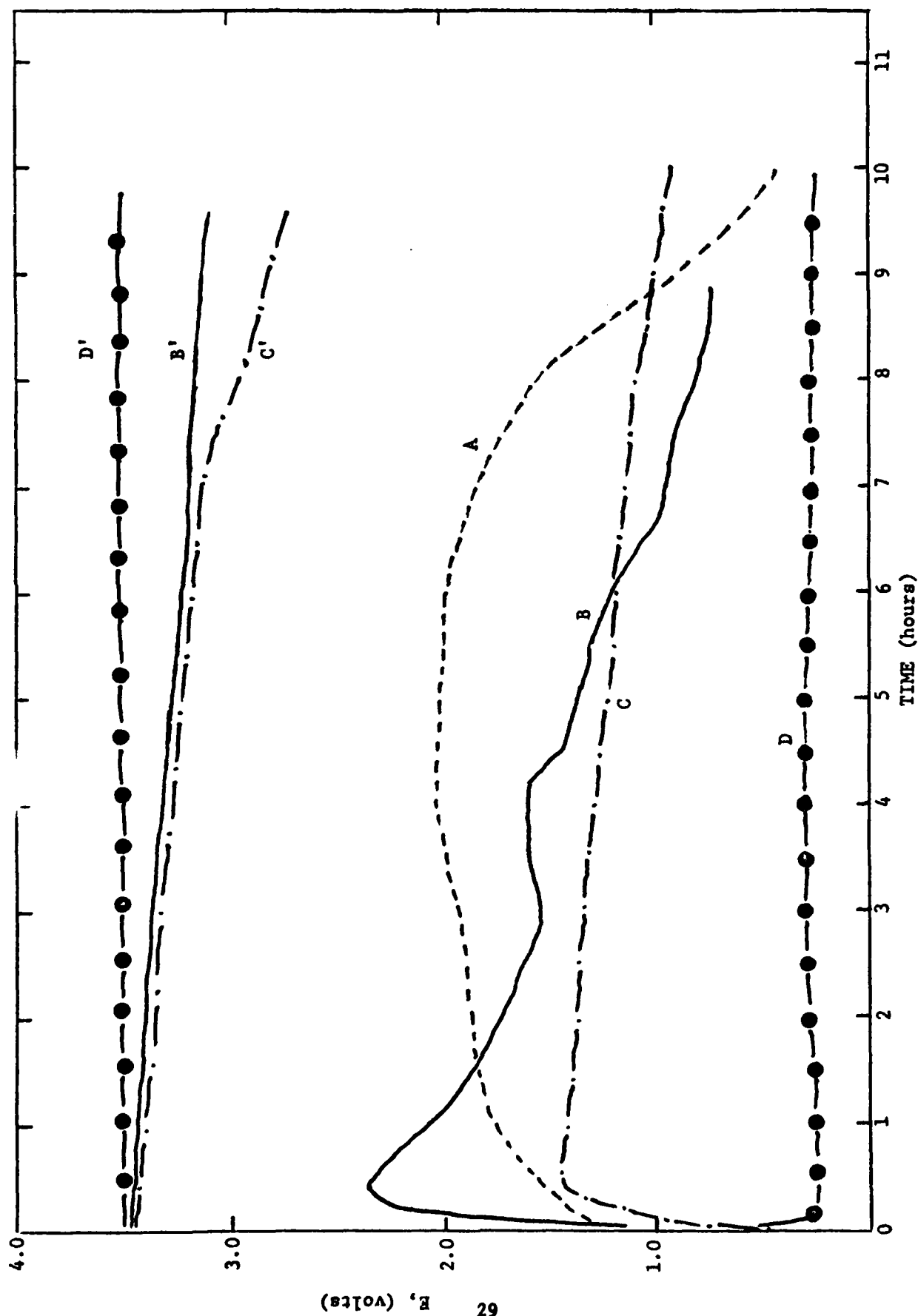Fig. 8: Oscillographic Trace of Voltage Delay Observed for Li/SOCl2 Cell After 16 Day Storage

28

Fig. 9: Room Temperature, 50Ω Load Discharge of Four Cells Stored at 160°F for ∿1 Week (A,B,C,D – cell voltage, B',C',D', respective C vs. Li reference potentials).
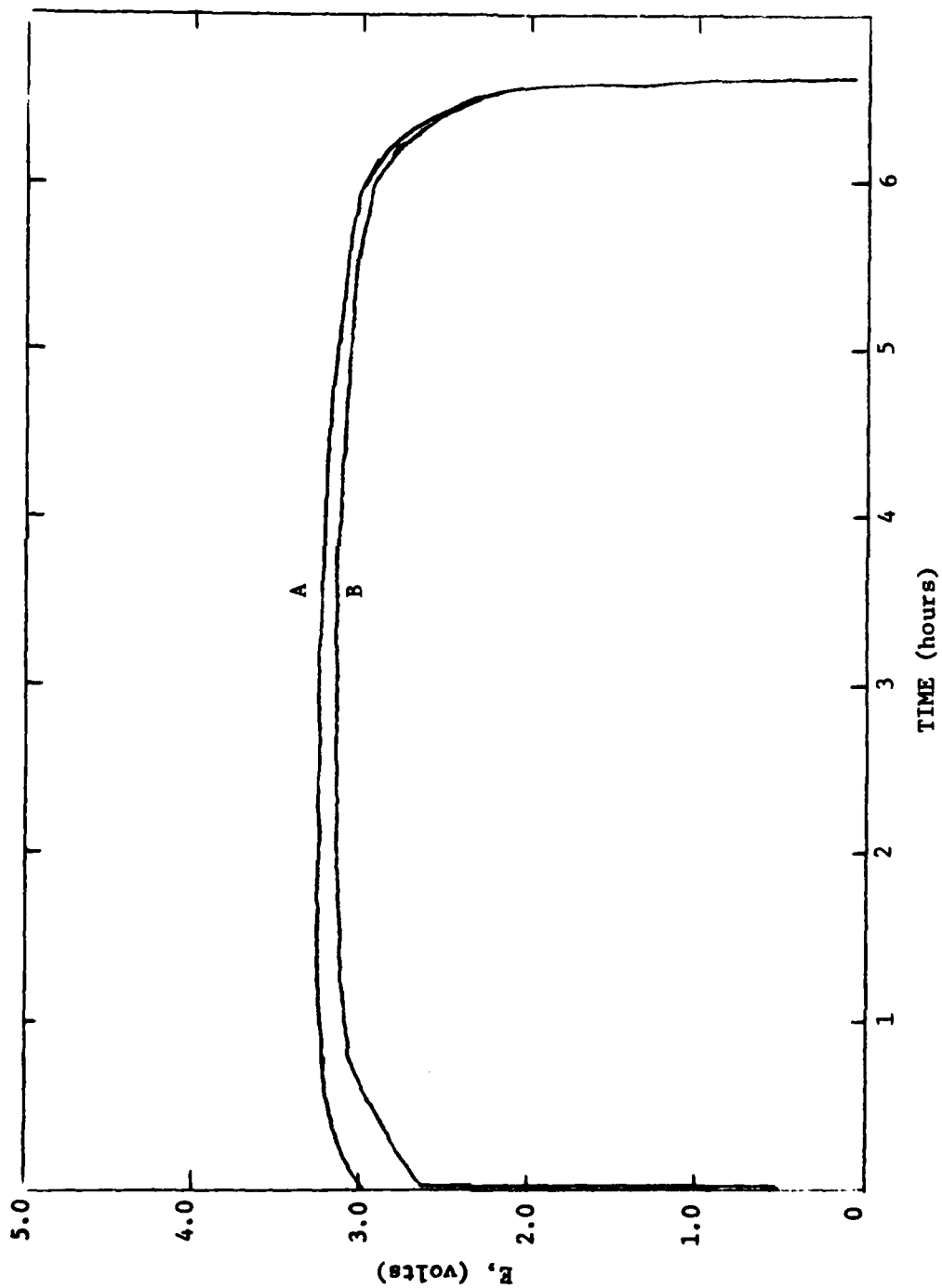
29

Fig. 10: Discharge Curve of Cell Stored at 160°F for 8 Days,
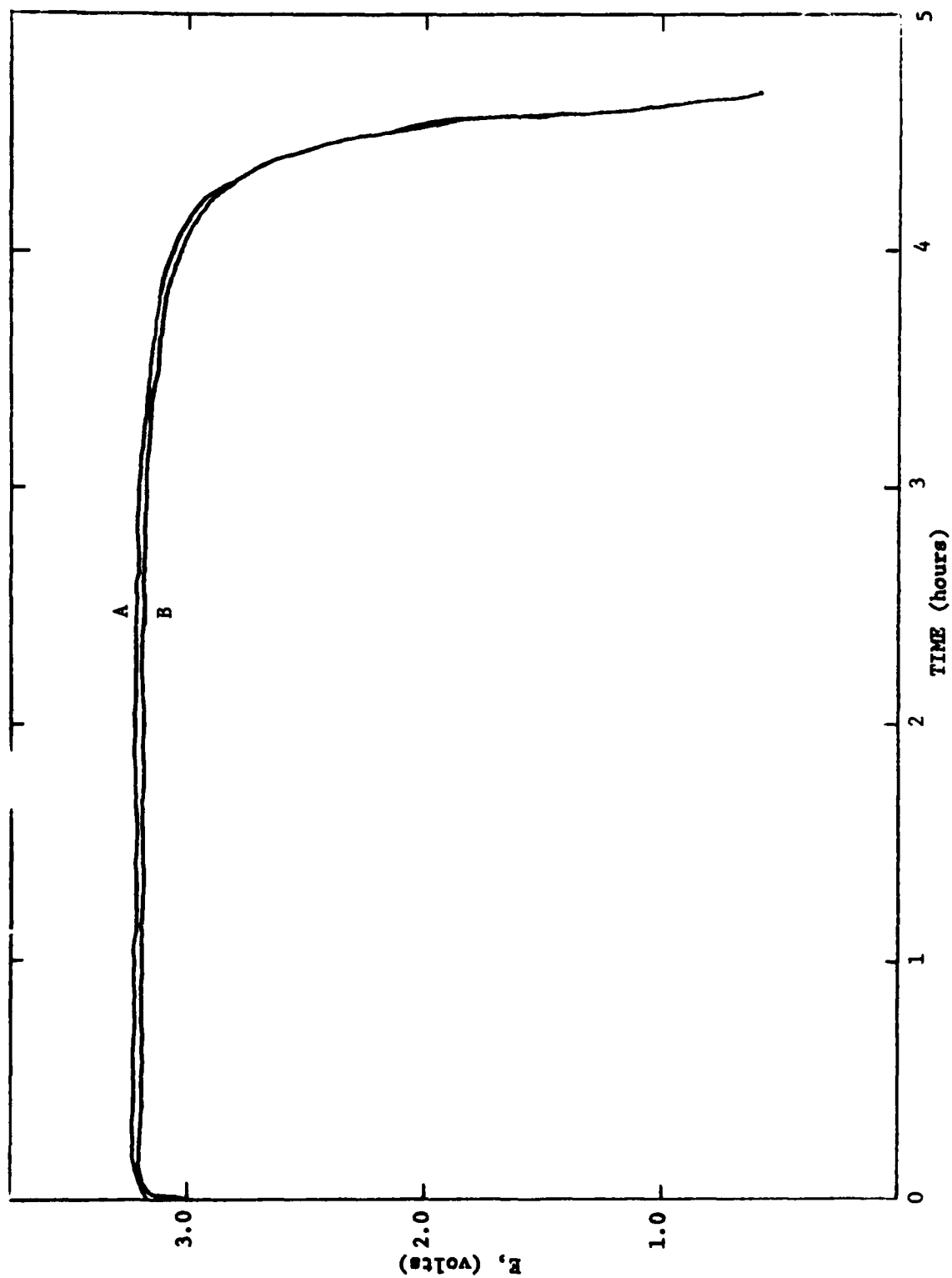Discharged at 160°F. A-C vs Li Reference Potential,
B-Cell Voltage

Fig. 11: Discharge Curve of Cell Stored @ 160°F for 15 hours, Discharged at 160°F.
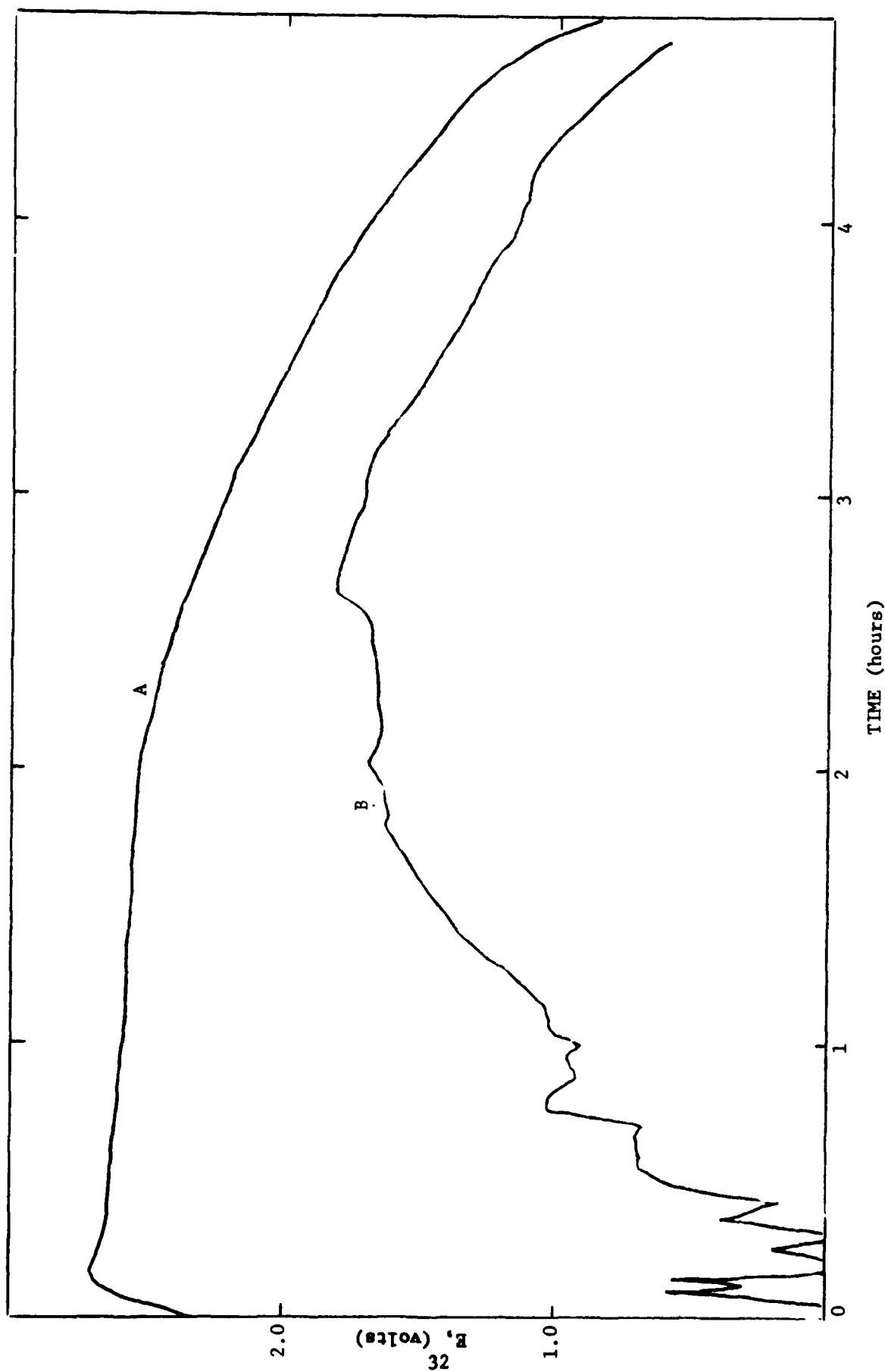A-C vs Li Reference Potential, B-Cell Voltage

31

Fig. 12: Discharge Curve of Cell Stored @ 160°F for 8 Days, Discharged at Room Temperature.
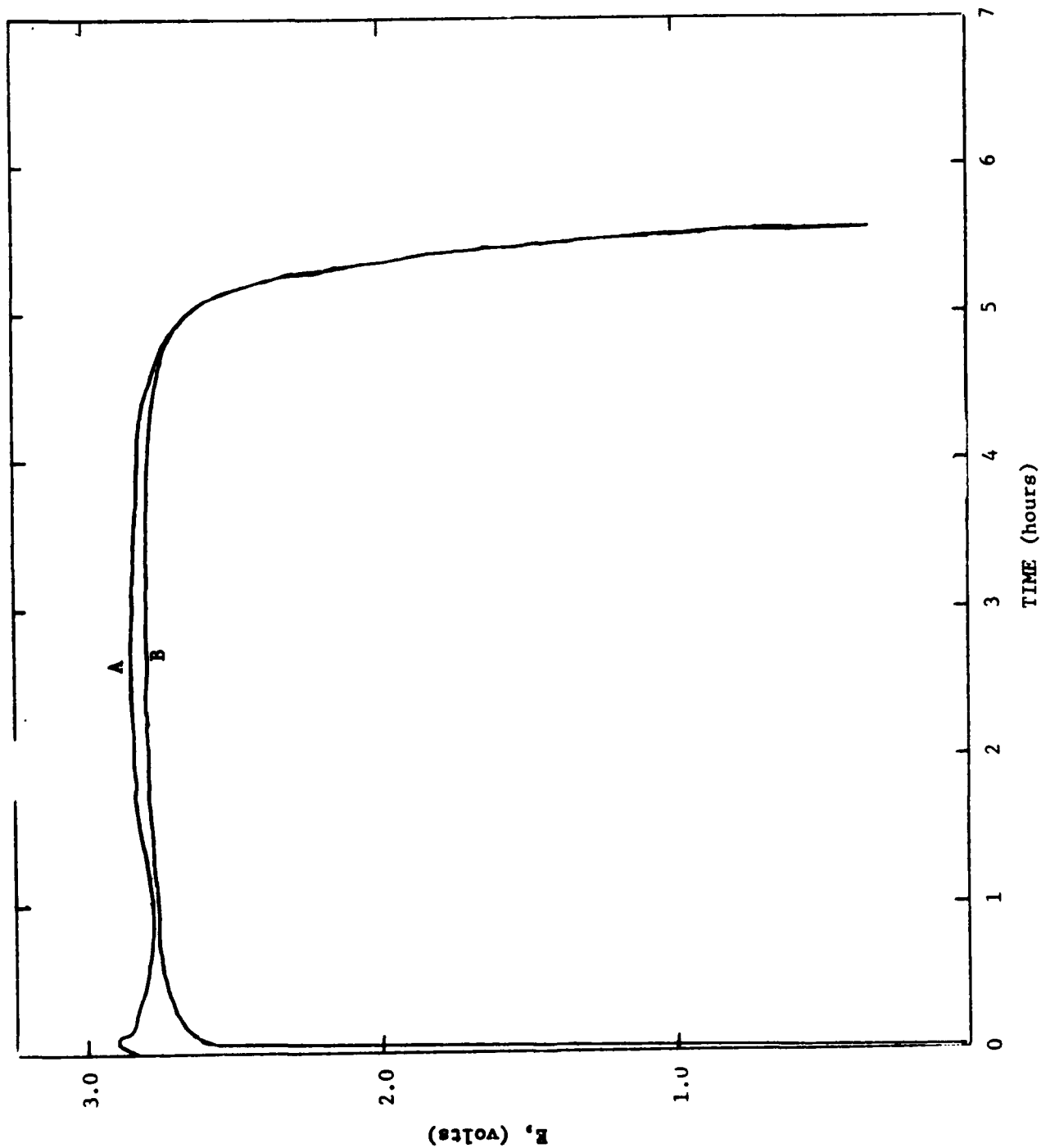A-C vs Li Reference Potential, B-Cell Voltage

32

Fig. 13: Discharge Curve of Cell Stored @ 160°F for 18 Hours, Discharged at Room Temperature. A-C vs Li Reference Potential, B-Cell Voltage

electrodes contribute to the voltage depression during further discharge. It appears that the polarization of the carbon electrode is caused by localized high current densities due to the uneven and very localized dissolution of the Li electrode. The few deep corrosion pits in the Li surface are clear evidence for the latter. Contrary to the previous cells, here we found no massive build-up of salts. With exception of the corrosion pits and along the edges, the Li was covered with a uniform brownish film.

3. Conclusion

From these results we have to conclude that room temperature discharge of $Li/SOCl_2$ cells after prolonged high temperature storage (160°F) can present a significant problem, and discharge at lower temperature will be even more difficult. The evidence indicates also that Li dissolves nonuniformly through the protective film, in localized fashion after film rupture or at inhomogeneities in the surface.

E. Lithium Corrosion and Voltage Delay

1. General

After storage at 160°F, experimental cells have shown severe voltage depression as a consequence of high Li electrode polarization. Further, upon visual inspection, thick layers of Li corrosion products (mainly LiCl) were found. This attack was much more severe than expected. In an attempt to pinpoint the cause for this behavior, we examined the effect of other metals of construction in electrical contact with the Li, as well as the possible effect of other impurities, by storing Li as elevated temperature in well-defined environments.

2. $SOCl_2$ Reduction on Substrate Materials

(a) Potentiostatic Measurements. A common procedure for testing compatibility of a material with a solution is to immerse it in the solution and to analyze for corrosion products. In this procedure, the potential of the material generally assumes its open circuit value. In a battery cell, it is also necessary to know the behavior as a function of potential. For example, if the nickel support screen of the Li electrode does not form a passivating layer (as does the Li itself), we can have a local cell between Ni screen and Li where $SOCl_2$ is reduced on Ni and Li corrodes. We carried out potentiostatic and galvanostatic experiments, generally starting from the open circuit value, to examine the electrochemical behavior of construction materials as a function of potential.

Typical current potential curves on Ni, stainless steel, and vitreous C electrodes are shown in Figs. 14-18. Current densities were recorded at five minute intervals as the substrate potential was
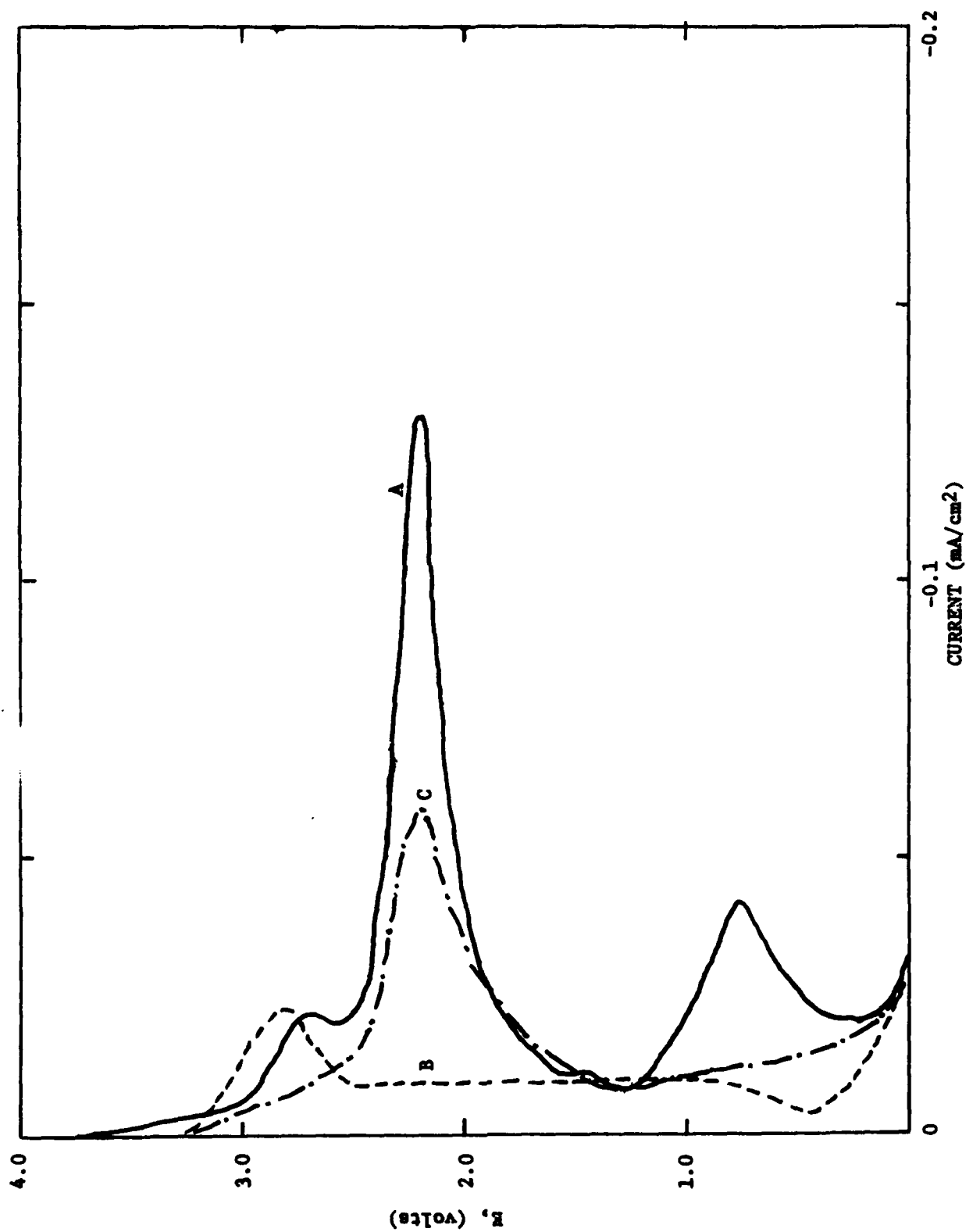
Fig. 14: Potentiostatic Reduction of $SOCl_2$ on Ni, Stepping 100 mV/5 min. (A - 1st cathodic scan, B - subsequent anodic scan, C - 2nd cathodic scan)
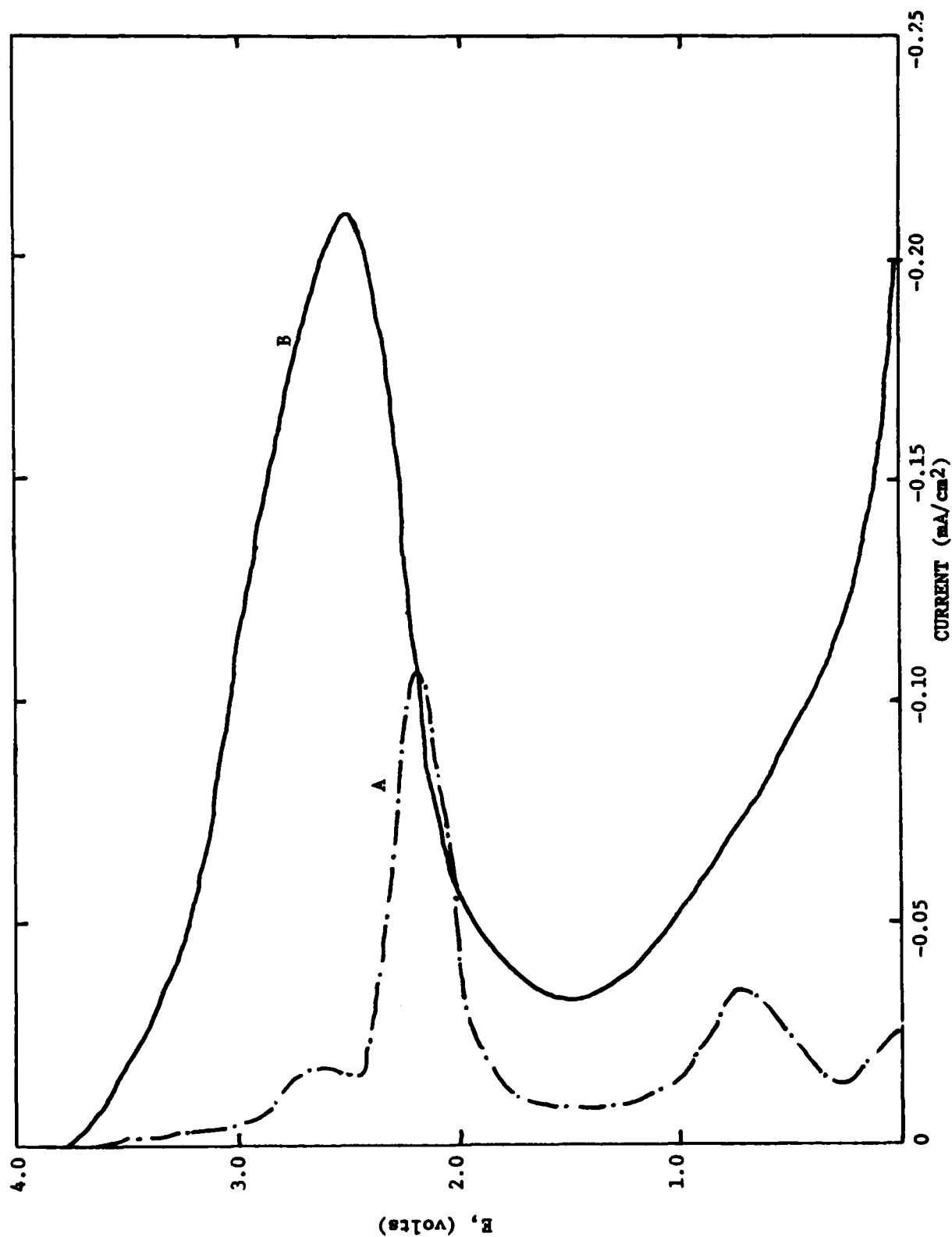
Fig. 15: Potentiostatic Reduction of SOCl2 on Ni, Stepping 100 mV/5 min. (A - 1.8M LiAlCl4 electrolyte, B - 1.8M LiAlCl4 plus 0.9M AlCl3 electrolyte).

36

Fig. 16: Potentiostatic Reduction of $SOCl_2$ on Ni at 160°F Stepping 100 mV/5 min.

37

Fig. 17: Potentiostatic Reduction of SOCl2 on Stainless Steel at Room Temperature, Stepping 100 mV/5 min.

Fig. 18: Potentiostatic Reduction of $SOCl_2$ on Vitreous Carbon Stepping 100 mV/5 min. (A – cathodic scan, B – subsequent anodic scan)
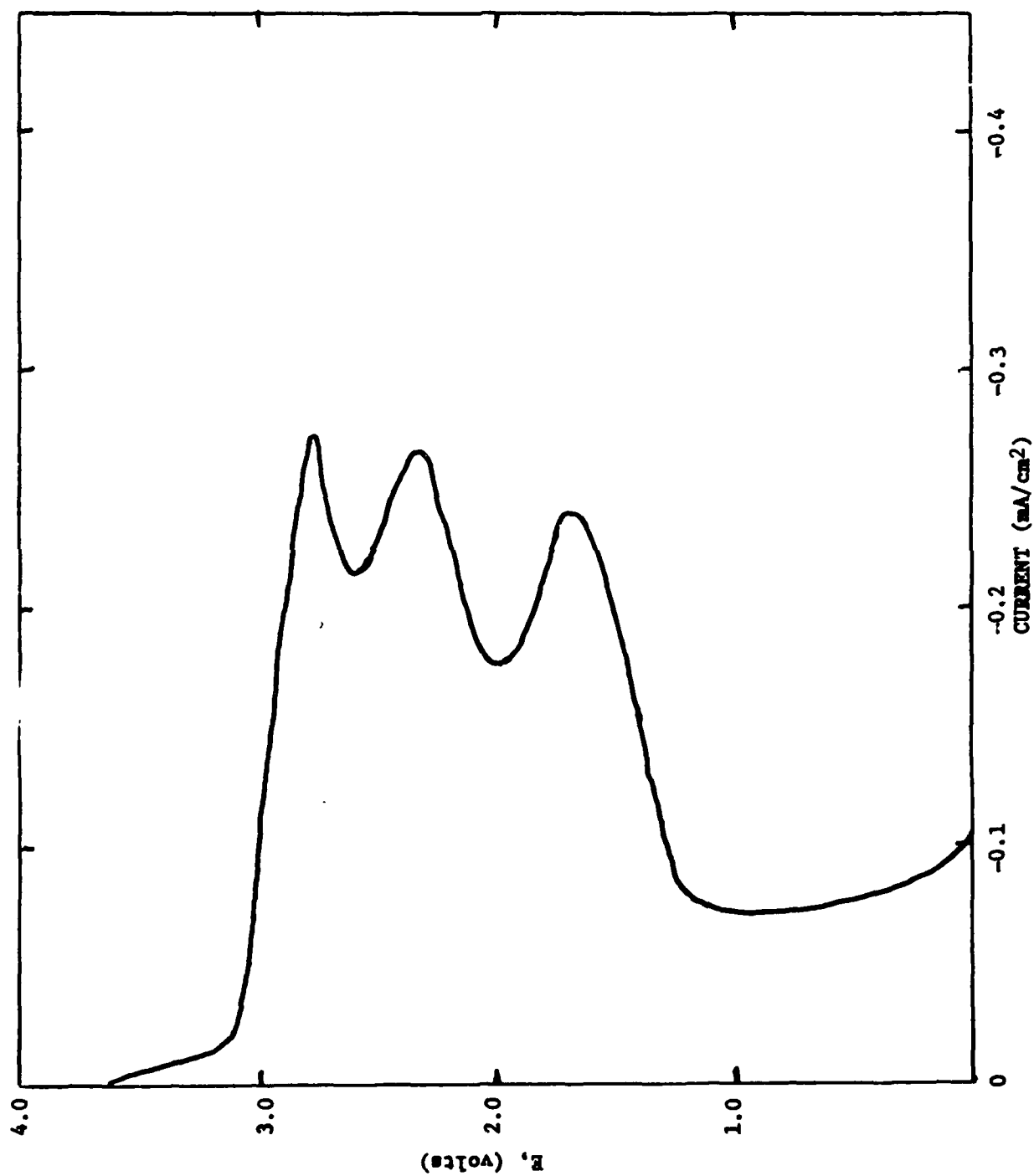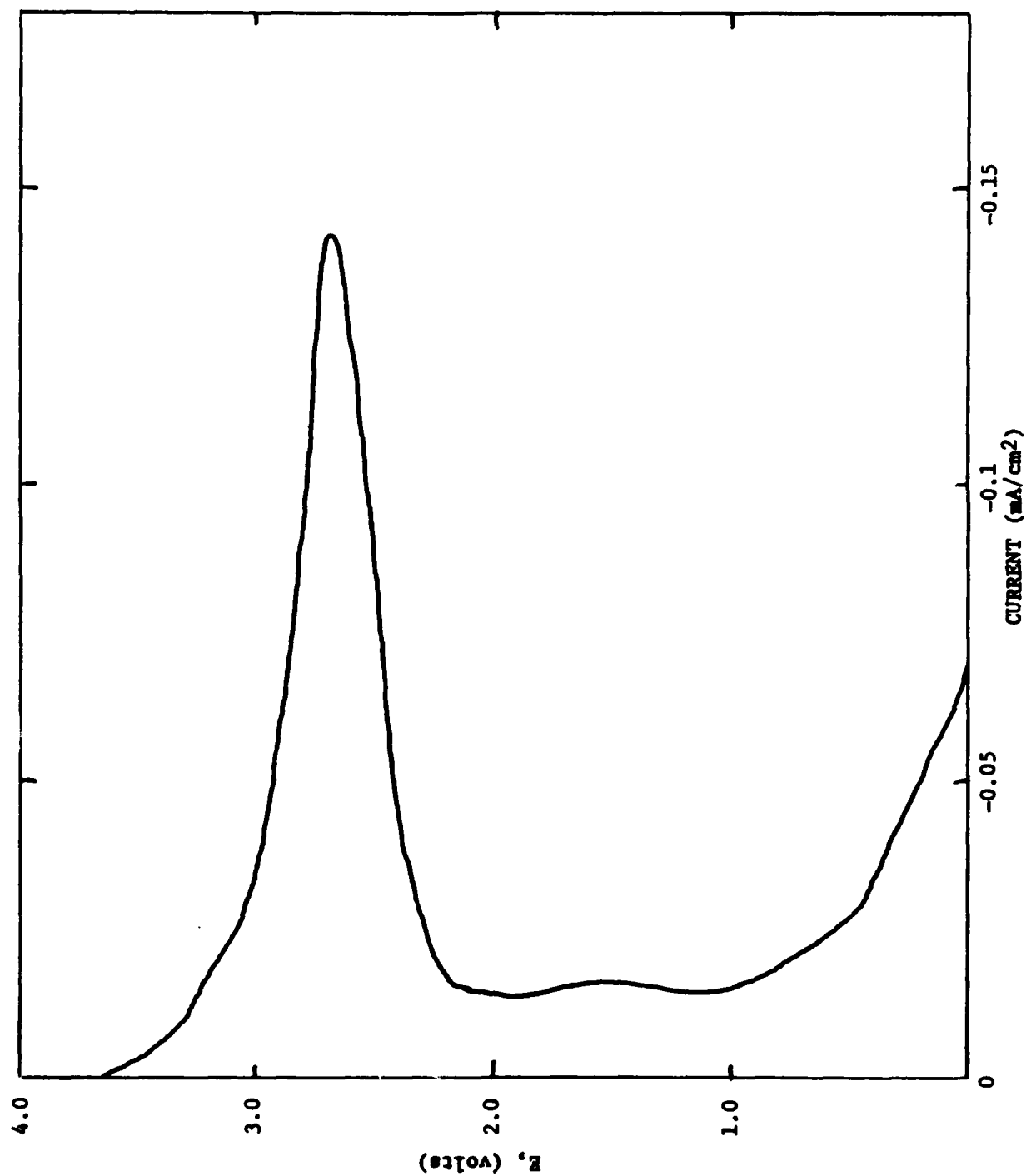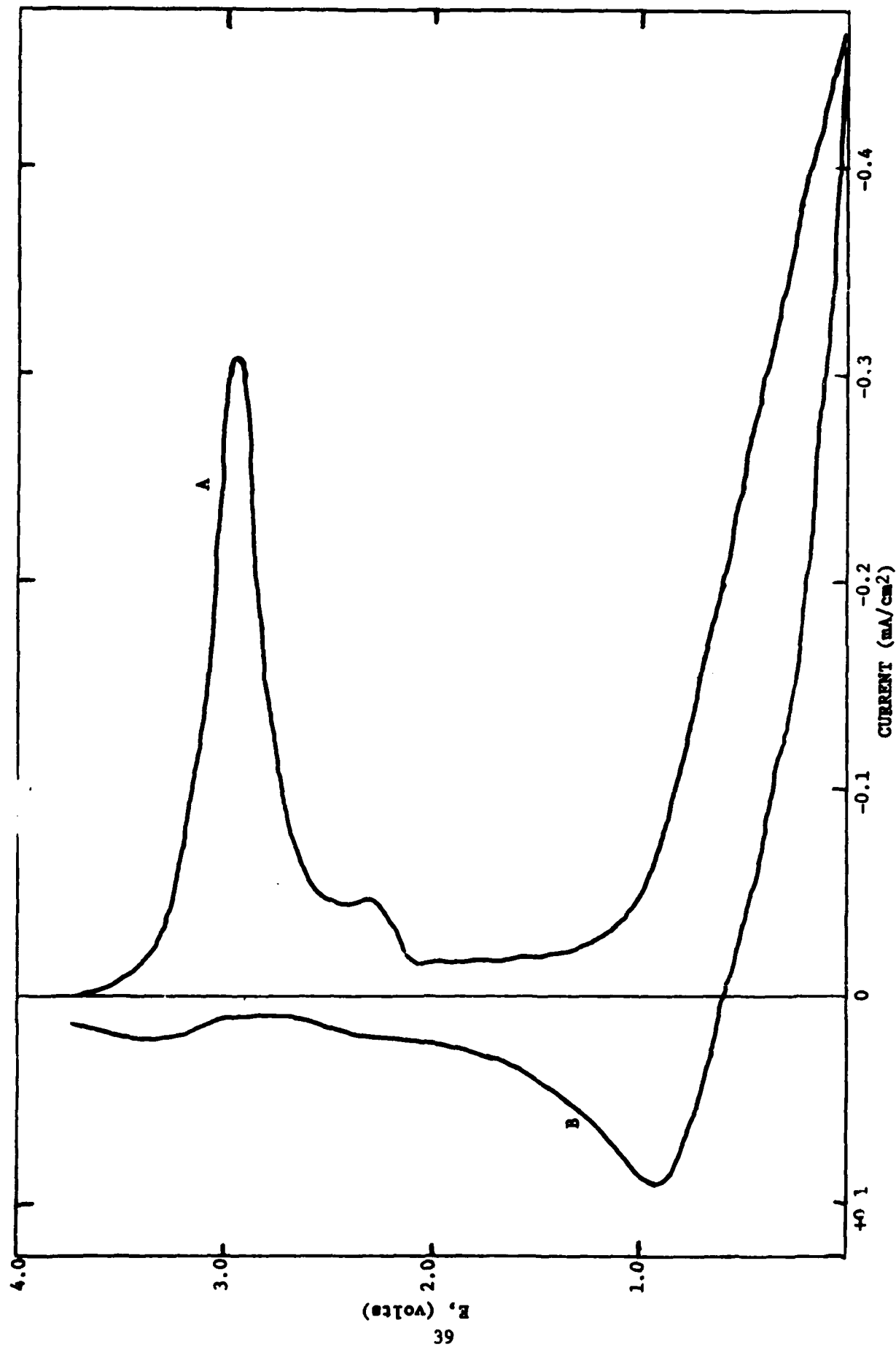
potentiostatically changed in 100 mV steps from the open circuit potential to the Li/Li$^+$ potential. The open circuit potential was between 3.7 and 3.8 V vs. Li/Li$^+$.

Ni shows three distinct reduction peaks (Fig. 14). The current decay at potentials negative to the main peak at 2.2 V can only be explained by the formation by a passivating or protective surface layer. The limiting diffusion current in solution is much larger (of the order of an A/cm^2). Despite passivation, there is a third reduction peak at about 0.8 V, and a slight current increase as the potential approaches that of Li. The following anodic cycle shows a constant cathodic current up to 2.6 V, then there is a reduction peak at 2.8 V. This apparently reactivates the surface, and on scanning cathodic the large peak at 2.2 V again appears. Following a cathodic sweep, the Ni electrode is covered with a film which, after washing with SOCl$_2$ and drying, has a white crystalline appearance. We have analyzed such films (see Table IX) and found LiCl as the major constituent.

If the protective or passivating film is essentially LiCl, this passivation should be practically nonexistent in a medium where LiCl is soluble. We therefore carried out a similar potentiostatic experiment in a SOCl$_2$, 1.8M LiAlCl$_4$, 0.9M AlCl$_3$ solution. The result is shown in Fig. 15. The reduction peak at 2.5 V is considerably larger and broader than in the standard electrolyte. At potentials between 1.0 and 2.0 V, however, the current again decayed to a value which is only approximately three times that in the standard electrolyte (0.025 mA/cm^2). The expected current for the diffusion-limited dissolution of LiCl by AlCl$_3$ is a factor of 1,000 larger. As the potential approaches that of Li, the cathodic current increases again.

Fig. 16 shows a quasi-stationary, current-potential curve on Ni at 160°F. Three distinct, relatively large cathodic current peaks are evident, followed by a region of reduced current. The latter is, however, significantly higher than at room temperature.

Stainless steel shows a behavior similar to Ni (Fig. 17). Here the main cathodic peak occurs at 2.7 V (the potential of the first small reduction peak on Ni) with a subsequent passivation, and a current increase close to the Li potential.

An equivalent investigation on vitreous carbon is shown in Fig. 18. The main solvent reduction occurs at about 3.0 V, with a "shoulder" at about 2.3 V, followed by a passive region. The marked cathodic current increase below 1.0 V leads to a material which can be reoxidized when the potential is swept from the Li potential to more anodic potentials. In Fig. 18 we see that there is an anodic current after about 0.6 V, which seems to be directly related to the previous cathodization. Evidently, this cathodization leads to a product which remains on the surface of the carbon. It could be due to the formation of a compound between Li and

the substrate, as has been frequently observed (10), or it could be due to a reduction product of $SOCl_2$.

(b) Galvanostatic Measurements. To obtain more quantitative data, galvanostatic $SOCl_2$ reduction experiments on nickel electrodes were carried out at various current densities. The discharge curve for 0.5 mA is reproduced in Fig. 19. The plateau regions labelled A, B, and C were typical. Table VIII gives a listing of the transition times T_A, T_B, and T_C and other data. From these data, it is apparent that at higher currents less charge is passed on each plateau. We know from our analytical data on Li^+ and Cl^- that LiCl precipitates where it is formed, and the efficiency of LiCl formation is independent of current density. Quantitative analysis (see Table IX) has shown that LiCl was formed on the Ni in an approximate ratio of 1 mole of LiCl per equivalent of charge passed. The amount formed, i.e., 60×10^{-6} micromoles per 10 cm^2 corresponds to about 10^3 monolayers or 1.2 microns. The voltage plateaus must then be due to processes which are concurrent with LiCl precipitation.

Referring to the final column of Table VIII, we note that plateau A does not correspond to a diffusion controlled process. The plateau B clearly shows a diffusion controlled transition time. The $i\tau^{1/2}$ values of the plateau C are irreproducible and may be governed by surface effects rather than diffusion.

From the equation

$$\tau^{1/2} = \frac{\pi^{1/2} nFCD^{1/2}}{2i}$$

we can estimate a corresponding solution concentration value. Assuming a one electron reduction (n = 1) and $D = 5 \times 10^{-6}$ cm^2 sec, we would require approximately a concentration of 14 mM or half that value for a two electron reaction. The transition times at the lower current densities are very long and can certainly not be explained by LiCl film formation. A further discussion, including the possibility of forming a partially soluble substance involving diffusion from the electrode into the bulk of the solution, will be postponed until measurements over a wider range of current densities (especially for shorter transition times) are available.

3. Li in Contact with $SOCl_2$

Relatively thick salt layers were found covering the Li surface after storage of cells at 160°F in stainless steel containers. We suspect that impurities, such as Fe from corrosion of the container, may be responsible for this. We therefore stored Li in contact with Ni and stainless steel, and Li together with carbon electrodes, in glass lined pressure vessels at 160°F to isolate the effect of the various components.
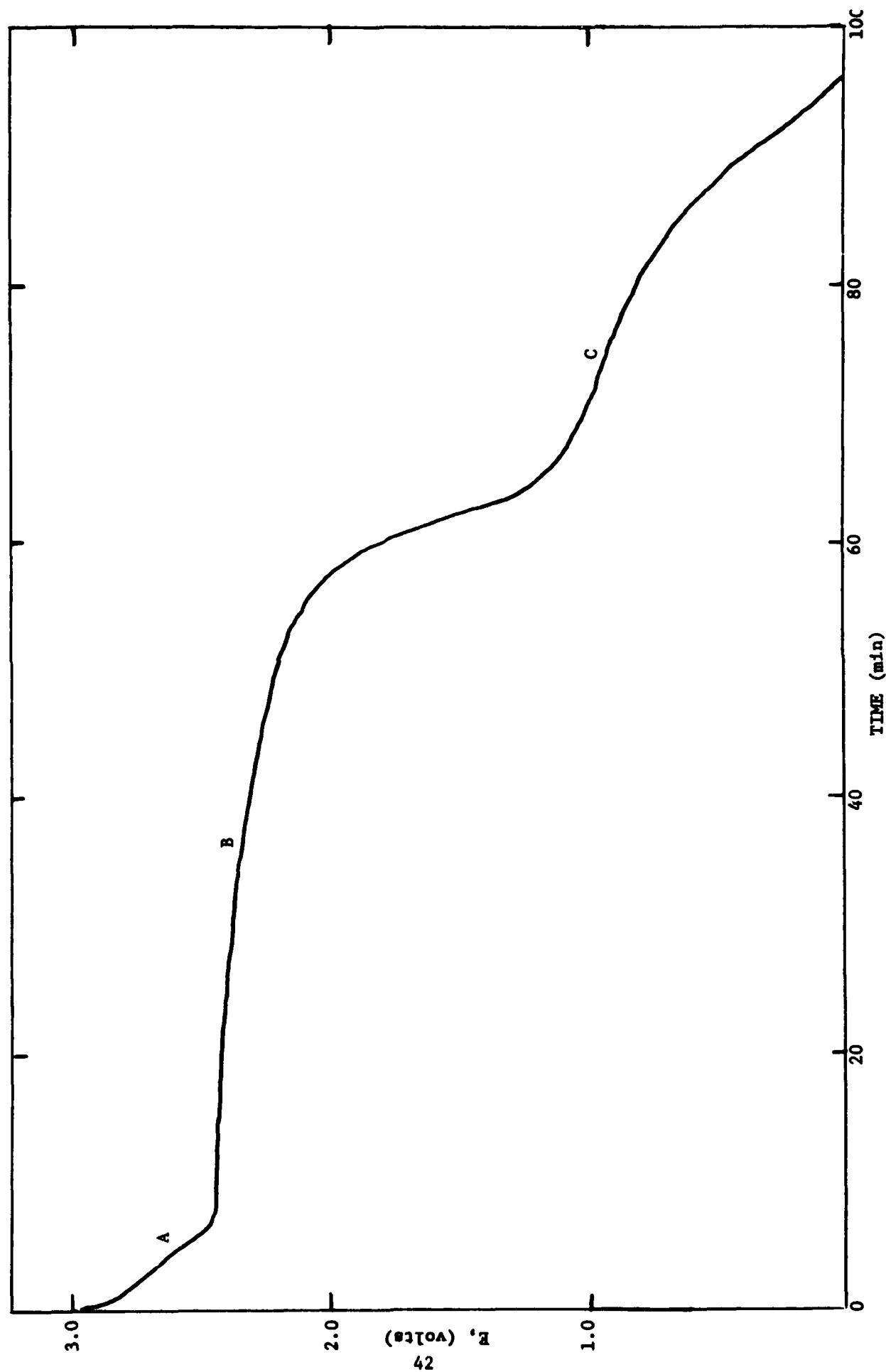
Fig. 19: Galvanostatic Reduction of SOCl2 on Ni at Room Temperature (current density 0.05 mA/cm²)

Table VIII: Galvanostatic Reduction of $SOCl_2$ on Nickel
in a Li/1.8M $LiAlCl_4$-$SOCl_2$/Ni Cell

Plateau	i	τ	$i\tau^{1/2}$
	(mA/cm^2)	(min)	(mA/sec$^{1/2}$/cm^2)
A	0.03	42.8	1.52
	0.05	6.2	0.96
	0.10	0.6	0.60
	0.10	1.0	0.77
B	0.03	137.5	2.72
	0.05	51.0	2.76
	0.10	12.0	2.68
	0.10	14.0	2.89
C	0.03	115.0	2.49
	0.05	19.5	1.71
	0.10	24.9	2.51
	0.10	5.5	1.82

Table IX: Analysis of Nickel Flag Electrodes for LiCl Precipitate

	Sample B2	Sample B1
Charge (coul)	5.17	6.41
Charge (microequivalents)	54.0	67.0
Li^+ (micromoles)	44 ± 5	44 ± 5
Cl^- (micromoles)	54 ± 5	53 ± 5

Storage of Li strips resulted in a pale brown coloration of the electrolyte, and a thin brown film on the Li pieces. The brown film was uniform from the bottom of each piece up to the electrolyte meniscus. No discoloration occurred above the meniscus line. Practically identical observations were made with Li connected to Ni or stainless steel and for the case where all cell components were stored together in a glass vial. In summary, we find that visible films do form on Li at 160°F, but to a lesser extent under relatively contaminant-free conditions.

In order to determine the electrochemical behavior of Li strips which had been stored at 160°F in $SOCl_2$ under controlled conditions (glass liner, no other materials such as Ni, C, etc.), they were incorporated into cells and discharged galvanostatically. An example of a partial discharge is shown in Fig. 20. Initially, the Li electrode polarizes severely and then recovers; however, it still remained significantly polarized. In addition to the continuous monitoring of the cell voltage and Li electrode potential vs. the Li reference electrode, we followed also the potential transients during current interruption. They suggest a small resistive component (a few ohms) and a large polarization upon current flow. After discharge, the Li surface appeared irregularly blotchy and pitted.

More extensive transient measurements were carried out on a complete "clean" cell (distilled $SOCl_2$, glass lined container) stored for 8 days at 71°C. The open circuit voltage after cooling to room temperature was 3.63 V and no potential was measured between the Li reference electrode vs. the Li working electrode. Upon initiation of a galvanostatic pulse of 70 mA (7 mA/cm^2) the cell polarized severely as shown in Fig. 21. The resistive component of this polarization, determined by an interrupter technique, can account only for a part of the polarization (resistance of 45Ω corresponding to a potential drop of 3.15 V out of ~22 V). The major part is due to activation and concentration over voltage. With time, the Li electrode polarization decreased and reached a fairly stable value of 6.0 V (ohmic resistance 28Ω). After a short time at open circuit, a distinct two step transient was observed (see Fig. 21). This behavior was at least qualitatively reproducible. The carbon electrode too showed a noticeable polarization which appears to be caused by relatively localized high current densities due to the spotty dissolution of the Li electrode. The pitted uneven surface of the Li is clear evidence for the uneven anodic attack. The rest of the electrode was covered with a thin brownish film. The build-up of a large Li ion concentration around the few active Li centers may account for the large polarization and could also explain part of the transient behavior after short open circuit periods. The data suggests further that the protective film is practically impermeable to Li and that anodic dissolution occurs only at locations of inhomogeneity or film rupture.

A more detailed discussion of these phenomena has to await further experimental results.
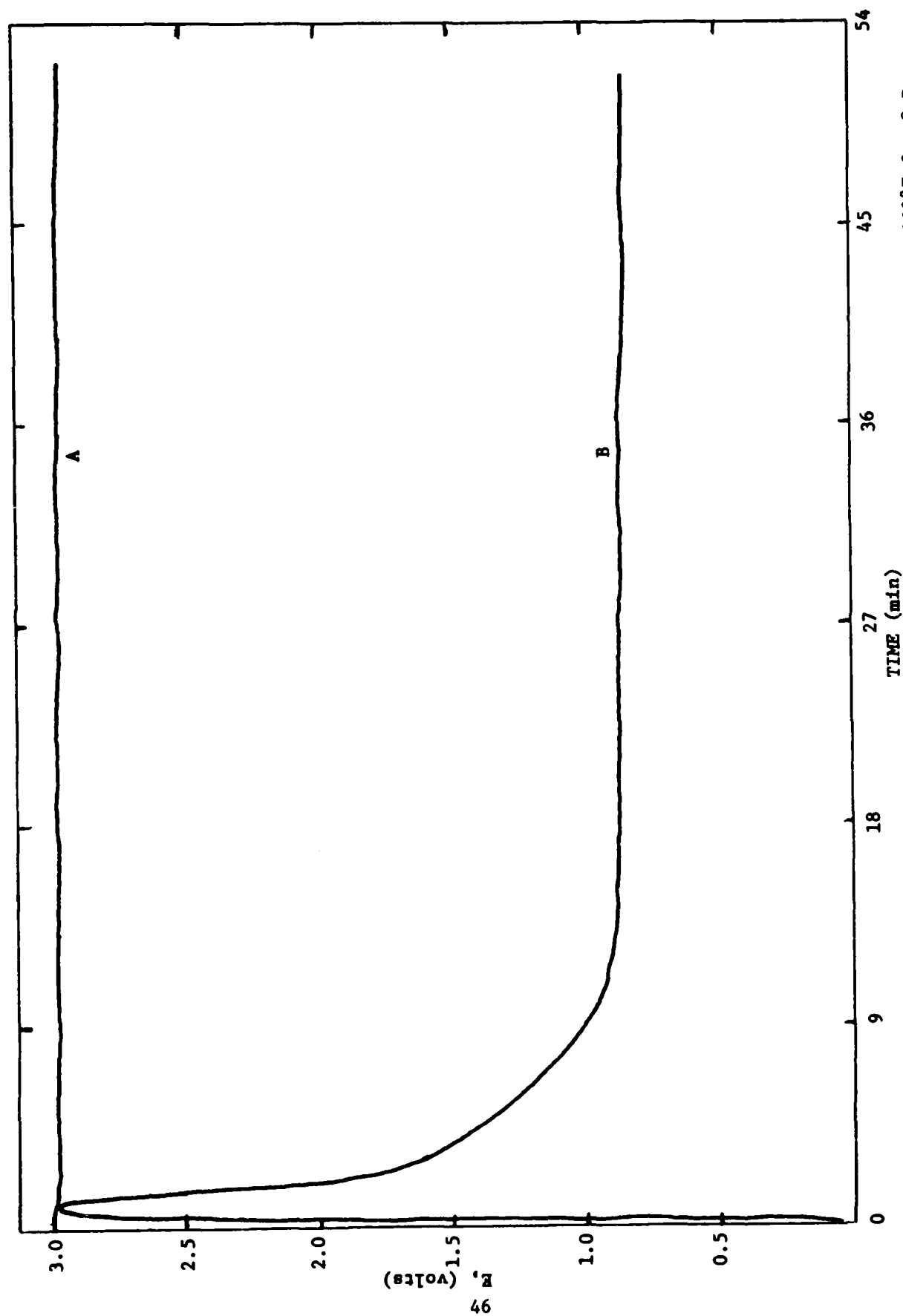
Fig. 20: Partial Galvanostatic Discharge of Cell Containing Li Anode Stored in Glass at 160°F for 8 Days. (A - C vs. fresh Li reference potential, B - Li anode potential vs. Li reference)
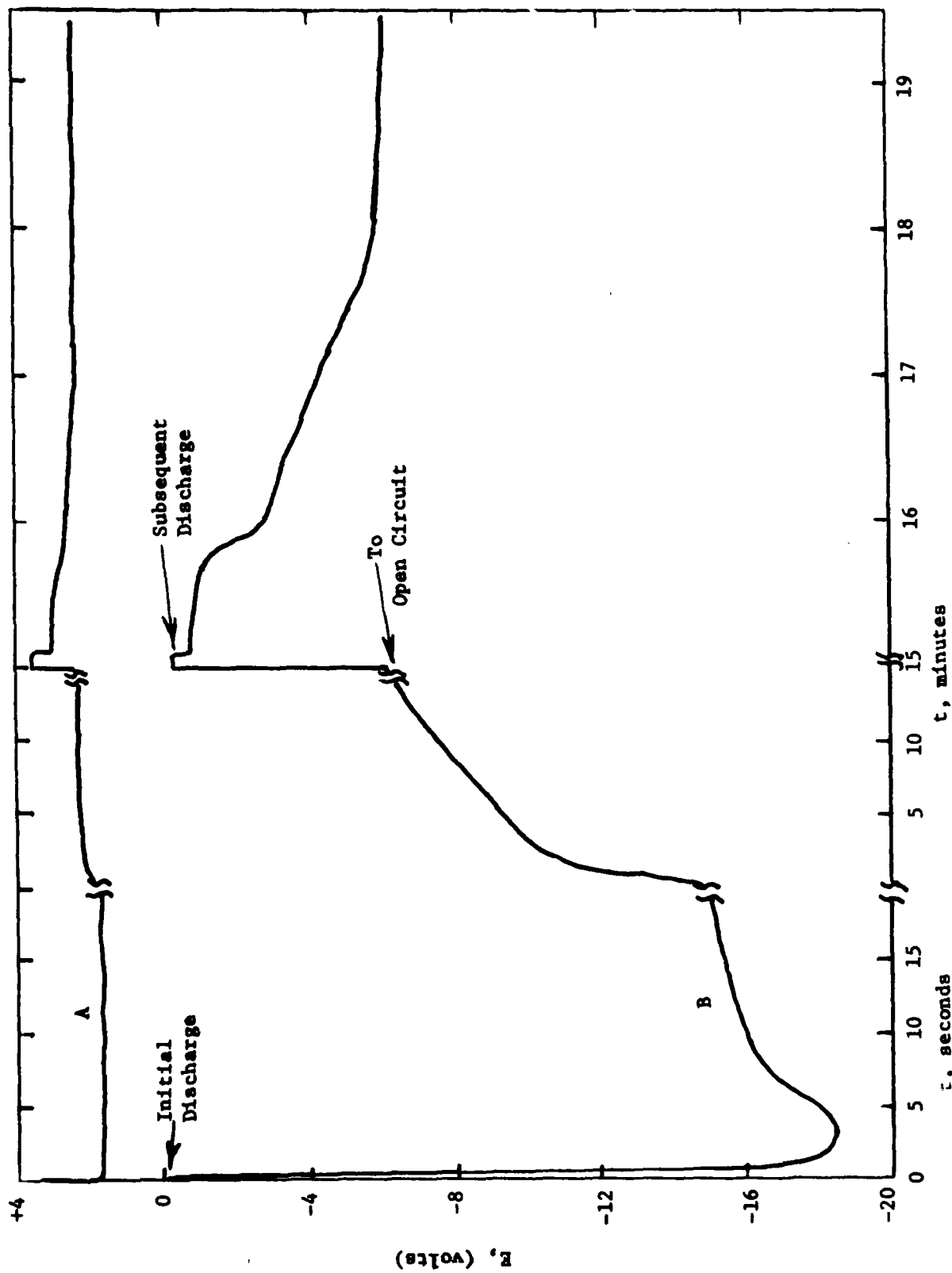
46

Fig. 21: Potential Excursions of C vs. Li Reference Electrode (A) and Li vs. Li Reference Electrode (B) During Room Temperature Discharge After 8 Day Storage at 160°F

47

4. Summary and Discussion

Lithium in contact with $SOCl_2/LiAlCl_4$ forms a protective surface layer and, in fact, it is this protective layer that makes the battery possible. In fresh cells, this layer does not interfere with battery discharge under normal discharge conditions. However, after storage, especially at elevated temperature, severe voltage delays and voltage depressions have been observed. Depending on the purity of the environment, films varying from tight brownish films to thick salt crusts have been observed on the Li surface upon storage at 160°F. LiCl is a major product in each case. The crystalline nature of the LiCl films has been vividly demonstrated by the scanning electron microscopy study of Dey (3).

We have shown that not only Li but also other materials such as Ni and SS form a protective surface layer at the Li electrode potential. This is of significant practical importance since screens of these metals are used as support for the Li electrode. This protective surface layer limits the reduction currents to low but still finite values (e.g., for Ni at 25°C $\sim$0.025 A/cm^2 after several hours; the current decays further at long times but c ly slowly). The residual current increases with temperature, and at 160°F it is about four times as large. Visible films are formed on the metal and the primary product is LiCl.

Indications are, however, that LiCl may not be the only film on the metal, and it may not be the main protective film: In an electrolyte containing a 50% excess of $AlCl_3$, thus solubilizing LiCl, observed currents are higher than in a standard electrolyte. But they are still about a factor of 1,000 less than should be expected if LiCl were the only protective film. The reduction of $SOCl_2$, and the formation of protective films on substrates (e.g., Ni, SS, C), is a complicated potential-dependent process. Once the film is formed, it limits the $SOCl_2$ reduction rate to very low values. There is evidence that the substrate can be reactivated by anodic polarization to about 3.0 V vs. Li. LiCl does not undergo any reaction in this potential range. Galvanostatic measurements suggest a diffusion-dependent rate of film formation.

Identical measurements cannot be carried out with Li, but if one assumes the formation of a protective film of similar nature on Ni and Li in $SOCl_2$, the experimental evidence indicates that LiCl is not the only film formed, and furthermore, that it is not the protective film.

IV. FUTURE WORK

Future work will emphasize further studies of the cell reaction and of film formation as it pertains to voltage delays on high temperature storage.

With respect to the cell reaction, we will extend the LiCl analysis to a broader range of operating conditions, especially to cells discharged at high rate. The quantity of S and the nature and amount of the gaseous component under various conditions will be established. Additional tests will be designed to determine possible other products.

The films formed on Li under various experimental conditions will be characterized with respect to their electrical, chemical and physical properties. We will investigate the effect of impurities and additions to the electrolyte. We will also explore the feasibility to control film growth by chemical modification of the system.

V. REFERENCES

1. W. K. Behl, J. A. Christopulos, M. Ramirez and S. Gilman, ECOM Report 4101, April 1973.

2. D. A. Skoog and J. K. Bartlett, Anal. Chem. $\underline{27}$ (3), 369 (1955).

3. A. N. Dey, Presentation at 26th Power Sources Symposium, Atlantic City, April 1974.

4. E. Brunneck, Dissertation T. H. Braunschweig, 1953.

5. H. Spandau, A. Beyer and F. Prengschat, Z. Anorg. Allgem. Chem., $\underline{306}$, 13 (1960).

6. A. N. Dey, Research and Development Report, ECOM 74-0109-1, for Contract #DAAB07-74-C-0109, July 1974.

7. M. Davis, H. Szkuta and A. J. Krubsack, "Chemistry of The Thionyl Halides," in Mechanisms of Reactions of Sulfur Compounds, Intra-Science Foundation, Santa Monica, Ca., Vol. 5, (1970).

8. W. K. Behl, J. A. Christopulos, M. Ramirez and S. Gilman, J. Electrochem. Soc. $\underline{120}$, 1619 (1973).

9. J. J. Auborn, K. W. French, S. I. Lieberman, V. K. Shah and A. Heller, J. Electrochem. Soc. $\underline{120}$, 1613 (1973).

10. A. N. Dey, J. Electrochem. Soc. $\underline{118}$, 1547 (1971).